

Javier García Díaz

VISUALIZATION OF MOTOR SYMPTOMS RELATED TO PARKINSON'S DISEASE USING WEARABLE SENSORS

Faculty of Medicine and Health Technology
Bachelor's thesis
May 2019

ABSTRACT

Javier García Díaz: Visualization of motor symptoms related to Parkinson's disease using wearable sensors
Bachelor's thesis
Tampere University
Biomedical Engineering
May 2019

Parkinson Disease (PD) is the second most common neurological disease after Alzheimer. There is a need for long term monitoring to determine with higher accuracy the stage of the disease and regulate the levodopa treatment. Current wearable technology can achieve this monitorization of the patient's daily life. Motor symptoms of the disease are the most evident and thus, the easiest to target and to relate to the stage of the disease. They are also the ones that suppose the highest impediment for the patients to perform their daily living activities.

In this study, motor symptoms are assessed via pressure sensitive insole and gyroscopic sensors placed on the wrists. Eight subjects were analyzed, four controls and four with different stages of PD, performing a 20-step walking test.

Pressure sensitive insole showed the transfer of force in the foot during the gait cycle. These signals showed the level of pronation and supination of each step. The force applied against the ground was reduced in subjects with PD, and specially seen in the toe-off phase which translate in a reduction in the ankle force. There was no apparent change in the step time in any of the signals.

Gyroscopic data evaluation consisted in time domain, frequency domain and spectrogram analysis and comparing the Root Mean Squared (RMS) value and entropy of the signals with the stages of the disease to see any correlations. These procedures were made with the signals measured in the three axes and with the calculated angular velocity vector module. The analysis showed that the tremor could be visualized and the effects of bradykinesia were visible in the signals while walking. RMS and Entropy values didn't show significance correlation between the stages of PD and their values with the exception of the RMS values of the signals in the Y axis and of the vector module. Tremors appeared in the frequency domain in the form of peaks at 5 Hz that were constant through the test, as shown by the spectrograms. The frequency domain of the vector module had the same peaks as the rest of the signals but at the double of their frequency.

Since all the signals correspond to a different person from simple tests, there was no way of assessing the effects of the different stages of the disease in the same individual over time.

Wearable technology supposes a good viable solution to the problem of long-term daily monitoring for patients with PD. Suunto Movesense ® gyroscope sensors and Smart insole Forciot ® suppose a good of non-invasive monitoring technology that can provide long term daily data with minimal discomfort while assessing motor disfunctions that alter the movements of a patient.

PREFACE

I would like to express my gratitude for the possibility to work in this project and for the supervision of the thesis by Milla Jauhiainen and Antti Vehkaoja. I would also like to thank the Käveli Project for providing the data necessary. The Käveli Project is a research consortium of Tampere University of Technology, Satakunta Hospital District, Orion-pharma Ltd, Suunto Ltd and Forciot Ltd.

Working on this thesis has given me a sense of the application of our current technology that can be applied to help monitor patients and benefit them with a more personalized treatment.

Tampere, 26 May 2019

Javier García Díaz

CONTENTS

1.INTRODUCTION	1
2.BACKGROUND	3
2.1 Parkinson's disease	3
2.2 Wearable sensors used for monitoring Parkinson's disease.....	5
3.MATERIALS AND METHODS	7
3.1 Study Material:	7
3.2 Methods:	8
3.2.1 Forciot data analysis:	11
3.2.2 Suunto data analysis.....	14
4.RESULTS AND DISCUSSION.....	17
4.1 Forciot Data Analysis	17
4.2 Suunto Data Analysis.....	23
4.2.1 Frequency domain.	24
4.2.2 Time-Frequency.....	26
4.2.3 RMS and Entropy.....	27
4.2.4 Vector module.....	29
5.CONCLUSIONS.....	33
REFERENCES.....	35
APPENDIX A: FIGURES.....	1
APPENDIX B: ETHIC, SOCIAL, ECONOMIC AND ENVIRONMENTAL ASPECTS.	
20	
B.1 Introduction.....	20
B.2 Impact description related with the project	20
B.3 Expanded analysis of some of the impacts.	21
B.3 Conclusion.....	21
APPENDIX C: ECONOMIC BUDGET	1

LIST OF FIGURES

Figure 1.	<i>Devices used: Suunto Movesense sensor (top left), Forciot Smart insole (top right) and cell phone (bottom) [8]</i>	<i>7</i>
Figure 2.	<i>First visualization of the data of patient Kav113. Time was in Unix units. Forciot data on top plots the 23 sensors together. Suunto data on the bottom plots the angular velocity in the three axes. Both plots on the left represented the first test and the ones on the right the second one.</i>	<i>9</i>
Figure 3.	<i>Difference between the raw (top) and cut (bottom) of the patient Kav110</i>	<i>10</i>
Figure 4.	<i>Example for subject Kav113 of how the data stored was represented. First and third figure come from Forciot device and second and forth from Suunto gyroscopes.</i>	<i>10</i>
Figure 5.	<i>Plot of the Suunto data separately so the angular velocity can be seen in the three axes.</i>	<i>11</i>
Figure 6.	<i>Original image of the pressure sensors (left), hand drawn grid over the original image (center) and the representation in a paper sheet (right).</i>	<i>12</i>
Figure 7.	<i>Example of a frame using the first colormap with a sample where all sensor signal is equal to zero giving as a result a binary image(left). The one on the corrected animation (right) has a range over 200 and the binary image only goes from -0.1 to 0.1.....</i>	<i>13</i>
Figure 8.	<i>Total Forciot input of all the sensors in the insole.</i>	<i>13</i>
Figure 9.	<i>Representation of the rotation around the three axes.....</i>	<i>14</i>
Figure 10.	<i>Data from Suunto represented on the left and the FFT on the right. X axis on top, Y axis on the center and Z axis on the bottom. Every FFT plot also has the RMS value of the signal.</i>	<i>15</i>
Figure 11.	<i>Spectrogram from the Suunto signal of subject Kav110. X axis on top, Y axis in the middle and Z axis in the bottom.</i>	<i>16</i>
Figure 12.	<i>Variation of the module of the angular velocity vector in time of patient Kav110 (top), FFT of the signal (middle) and its spectrogram (bottom). Entropy and RMS values shown on the top graph.....</i>	<i>16</i>
Figure 13.	<i>Total force signal from the Forciot insole of two full gait cycles of control subject Kav138. The two peaks corresponding to the heel strike take values of 536 and 540 N and the ones corresponding to the toe-off reach 708 and 722 N.....</i>	<i>18</i>
Figure 14.	<i>Force from each sensor of the Forciot insole of two full gait cycles of control subject Kav138 (left) and sensor placement on the insole (right).</i>	<i>19</i>
Figure 15.	<i>Total input from Forciot insole of all four subjects presenting PD disease. Kav110 (UPDRS 1.5) on the top left, Kav096 (UPDRS 2.5) top right, Kav112 (UPDRS 3) bottom left and Kav042 (UPDRS 4) bottom right.....</i>	<i>20</i>
Figure 16.	<i>Force from each sensor of Forciot insole of all four subjects presenting PD disease. Kav110 (UPDRS 1.5) on the top left, Kav096 (UPDRS 2.5) top middle, Kav112 (UPDRS 3) bottom left, Kav042 (UPDRS 4) bottom middle and location of every sensor in the insole (left).</i>	<i>21</i>
Figure 17.	<i>Three complete gait cycles from subject Kav114. AV measured around X (top), Y (center) and Z (bottom) axes.</i>	<i>23</i>
Figure 18.	<i>Time (left) and frequency (right) analysis of angular velocity data around the three axes from subject Kav112.</i>	<i>26</i>

Figure 19.	<i>Spectrogram of the angular velocity signal from subject Kav112.....</i>	<i>27</i>
Figure 20.	<i>Analysis of the angular velocity vector module for control subject Kav113.....</i>	<i>30</i>

LIST OF TABLES

Table 1.	<i>Table containing all the subjects, first four with already diagnosed PD and the last four are controls.....</i>	<i>8</i>
Table 2.	<i>Table containing the average step time, average max input and the average integral per step. The number (Forciot 1-2) refers to the test number.....</i>	<i>22</i>
Table 3.	<i>RMS values of every patients Suunto data. The number (Suunto 1-2) refers to the test number.....</i>	<i>28</i>
Table 4.	<i>Spectral entropy of every patient's Suunto data. The number (Suunto 1-2) refers to the test number.</i>	<i>29</i>
Table 5.	<i>Table containing the RMS and entropy values for the module of the angular velocity vector for every test.</i>	<i>31</i>

LIST OF SYMBOLS AND ABBREVIATIONS

PD	Parkinson's Disease
TRAP	Tremor, Rigidity, Akinesia and Postural instability
UPDRS	Unified Parkinson's Disease Rating Scale
MDS	Movement Disorder Society
PET	Positron Emission Tomography
SPECT	Singel Photon Emision Computerized Tomograpy
CT	Computerized Tomography
FOG	Freezing Of Gait

1. INTRODUCTION

Parkinson's disease (PD) is the second most common neurodegenerative disorder after Alzheimer's disease with a lifetime incidence of approximately 2 percent, currently affecting around 10 million people [1]. The prevalence of the disease in industrialized countries is approximately 0.3% looking to the whole population and around 1% of third age which means people over 60 years old. PD is an age-related disease: In population under 50 it is very uncommon and for people in the highest age groups it can get up to 4%. [2]

It is significantly difficult to diagnose PD when the disease is still in its early stages and if it's only assessed in a single point in time. Diagnosis accuracy can be improved by long-term follow-up, when the symptom progression and effects of levodopa therapy can be monitored [2]. Early detection is key to develop an effective treatment, monitor the symptoms of the beginning of the disease and treat the secondary health issues that come with it.

Issues monitoring the disease come from the variability the motor and non-motor impairments from each patient and thus, they should be evaluated in the context of each patient's lifestyles needs and goals [3]. The progress of the disease has different timelines from person to person and there is a daily change in the symptom manifestation. The severity may vary from day to day or even in the same day. The problem with these changes is that they are difficult to monitor during relatively short appointments at the neurology policlinic. During these follow ups, symptoms are visually analyzed by the neurologist, so there is no objective way of monitoring the amount or severity of the symptoms and the diagnosis relies entirely on the specialist. Since the monitoring of the PD patients is based on subjective assessment, the full range of symptoms may not be visible during short appointments. Thus, objective home-monitoring systems for Parkinson's disease to maintain and effective treatment plan are needed.

Wearable sensors can provide significant information for remote monitoring of PD patients. That way, every time there is a deterioration on the symptoms, the frequency and the intensity of them can be recorded to assess the variation of the health, how he/she is responding to the treatment dosage and if any increase/decrease of it is needed. Thus, an improvement of the monitoring of the patient is needed and developing new cost-

effective, non-invasive technology to do so is essential to improve patient's life quality and extend his lifetime.

The Käveli project made a study during 2018 of monitoring PD patients using wearable technology in the form of a pressure detection insole, gyroscopic sensors attached to the wrist and a smartphone. This thesis aims to visualize the data from a 20-step test performed by the subjects. The goal was to interpret the signals from 4 subjects in different stages of PD and 4 controls, observe how the development of the disease affects the signals and extract some features that can be used to distinguish the symptoms and their severity in order to make the data understandable by healthcare professionals.

Data was collected from the insole and the gyroscopic sensors previous to this thesis and it was read thanks to a code provided in advance by Ville Vianto. The processing and analysis of the signals was done independently during the thesis. Pressure data was analyzed in time and animations were made to visualize the force transfer through the insole. Angular velocity data was analyzed both in time and frequency and extra features were extracted such as RMS and spectral entropy values. The results obtained with PD subjects were compared to the controls to see how the signals were affected by the different stages of the disease in different subjects.

The work presented in this thesis starts with the background including the Parkinson's disease and supervision techniques using wearables. The second section explains the materials and methods organized according to the type of data that was being processed. The third section discusses the results obtained and argues about the origin of the signal variation. This section is divided in two parts: the first one describes the results of the pressure sensors and the second one of the angular velocity signal. This last part is again divided in several sections depending on the type of analysis performed. The last part summarizes the thesis and adds a conclusion to it.

2. BACKGROUND

2.1 Parkinson's disease

There are four main dysfunctions associated with PD: Tremor at rest, Rigidity, Akinesia (or bradykinesia) and Postural instability. All together, they can be named as *TRAP*. Parkinsonism has also other features such as freezing due to motor blocks and fixed posture [3]. PD can be defined, if only looking to the motor symptoms, as bradykinesia in combined with rigidity, tremor at rest or the three of them together [3].

Postural tremor has been seen in many PD patients and it has the exact same features of the essential tremor or rest tremor but sometimes it can be more disabling than the other two and can be considered one of the first features manifested by the disease [3]. Rest tremor varies from 4 to 6 Hz and it happens only in a fully resting limb. It usually stops when the movement starts. Rest and kinetic (during movement) tremors by themselves are not enough to diagnose PD.[3]

Rigidity is characterized by increased movement resistance independently to its velocity ("lead-pipe" resistance) [3], usually together with the "cogwheel" phenomenon [3]. "Cogwheel" phenomenon occurs when the muscle is stiff, but, when at rest, tremors happen [19]. In the end, rigidity can cause a failure to relax. If "cogwheel" phenomenon occurs without the "lead-pipe" resistance, it is not considered as rigidity [3]. One instance in which it is manifested is in the freezing of gait (FOG). FOG is defined as "brief, episodic absence or marked reduction of forward progression of the feet despite the intention to walk." [22]. This includes problems initiating gait, problems turning and "destination hesitation" and times were the movement is achieved by dragging the feet and moving them few centimeters or even millimeters [22]. Something special about FOG is that PD patients with FOG can overcome it with the aid of auditory or visual cues [23].

Bradykinesia refers to slowness of movement and lower amplitude and speed [3]. It is the most characteristic clinical feature of PD. It includes difficulties with planning, initiating and executing movement and with performing sequential and simultaneous tasks. The reduction in the pace of the movements when performing daily living activities and the stretching of the reaction times can be seen as an initial manifestation of this specific feature. Other manifestations include loss of spontaneous movements and gesturing, drooling because of impaired swallowing, monotonic and hypophonic dysarthria, loss of facial expression (hypomimia), decreased blinking, and reduced arm swing while walking. This feature is the easiest to assess without any specific tests or formal neurological

examination [4]. The evaluation of bradykinesia commonly consists in several motor tests that have the patients perform fast repetitive movements according to the MDS-UPDRS. This task can be hand movements, pronation and supination or finger, toe and foot taps [3] Most likely slowness and a decrease in the amplitude of the movements would be observed. [3]

Electromyographic analysis revealed that bradykinesia causes an inability to stimulate the muscles needed to provide sufficient strength to start or keep large fast movements. These large movements are accomplished by multiple stimulation of the agonist muscle as a consequence of the reduction of the electromyographic activity caused by PD. [5]

Late stages of the disease can cause the loss of postural reflexes that usually causes postural instability and it mostly happens after other parkinsonism features have already appeared. There is a test that has the patients being pulled back and forth called “pull test”. It tests how the patient respond in terms of retro/propulsion to try to counteract the movements. The abnormal postural response would consist in taking more than two steps to keep balance or the absence of any response at all [3]. Postural instability is not considered as criteria for Parkinsonism by the Movement Disorder Society (MDS) [3].

Rather than tremor or bradykinesia, postural instability is the main cause of falls in PD patients [6] and thus, can lead to injuries such as broken hips. This PD feature is influenced by many other factors such as sensory changes related to age, other PD features, the capability to process different sensory inputs (kinesthesia) and orthostatic hypotension. [3] [7]

There are some abnormalities that can cause the same motor symptoms observed in PD. The detection of this anomalies would rule out the possibility of PD. Some of these features would be cerebellar abnormalities, absence of response to high levodopa dosage, motor symptoms showing exclusively to the lower limbs, etc. [3]

PD patients are usually capable to perform simple tasks relatively easy but, when trying to perform simultaneous or motor cognitive tasks, they usually find it more difficult. Such is the case when walking straight in contrast with, for example, walking and turning. Overall there is a difficulty in movement performance which becomes slow and under scaled in size. This is called hypokinesia [12]. Hypokinesia, akinesia (absence of movement) and dyskinesia (involuntary movements) affect PD gait. The first one is much more common to produce gait disturbances than the other two [12].

One big problem that hinders early diagnosis is that the patient is only referred to the neurologist only when the symptoms are actually visible for themselves or family members. A diagnostic test for PD that is trustworthy and easily applicable is not yet available.

Motor symptoms are the most common and detectable signs that can be assessed for both diagnosis and for evaluating the effectiveness of the treatments.[3]

Advance medical imaging techniques such as SPECT (Single Photon Emission Computerized Tomography), PET (Positron Emission Tomography) or CT (Computerized Tomography) are useful to diagnose PD and rule out other possible cause of the symptoms, such as brain tumors, but they require specific settings only achieved in special places such as hospitals. With time these techniques have become more advanced and more accessible to use but they are still not useful enough for population-based epidemiological research. This is the reason why the clinical symptoms are still the base of PD epidemiological studies. Therefore, at least two out of the four main motor symptoms are required to diagnose parkinsonism by the current criteria standards. [2]

Doctor's appointments are usually short and due to the variation on the symptoms mentioned before, he may not get the full scope of the disease. During these meetings, the doctor tries to get some feedback from the patient about his daily life to get some information about how the treatment is working. In some cases, patients may have memory issues or other cognitive problems and may struggle to do so.

Treatment assessment has the same problem since it sometimes depends on how the symptoms are described by the patient and how the doctor sees the patient. Therefore, there is no way to mathematically optimize the medication timing. This is why remote monitoring could give additional information useful to modify this timing.

2.2 Wearable sensors used for monitoring Parkinson's disease

Previous analyses of PD gait show specific features of the distorted walking. Reduced or absent arm swing, reduced trunk rotation, forward stooped posture, slowness, reduced footstep size, decreased ground clearance, excessive hip and knee flexion and reduced amplitude motion at the hips, knees and ankles are some of the hallmarks of a parkinsonian gait [13] [14]. Reduction of stride length is the most prominent feature of the gait of PD patients which comes together with lower walking speed and a longer duration on the double-support phase [15]. Several studies proved that patients were able to correct spatiotemporal and kinematic parameters with the aid of external cues but the forces measured stayed abnormal: at push-off, the ankle power generation stayed reduced, however they didn't use wearable sensors but rather video recordings and pressure plates [15] [16].

There are many examples of the use of wearable devices to assess PD motor symptoms. For example, there is a study that analyzed the plantar force distribution in PD patients

using a pressure sensitive insole. When comparing the data to the controls, they noted that there was an increase at the midfoot load in the patients affected with the disease [17]. In other instances in which the focus of the study has been detecting FOG using inertial sensors mounted on wrists and ankles [20][21][25].

Tremor effects have been measured several techniques. Rissanen et al. extracted several characteristics from this feature using inertial sensors attached to the wrist [11]. Another type of analysis was performed by Donghee Son et al. [24]. They used nanotechnology-based patches that sensed muscle activity. These devices were used to detect different tremor frequencies in PD patients to help monitoring the disease.

Inertial sensors (accelerometers and gyroscopes) have also been used to detect the effects of bradykinesia in several studies. These have been placed in several body parts such as the lower back, ankles and wrists [25][26][27]. Triaxial accelerometer measurements have been utilized to assess bradykinesia in the sleep and showed that the motor features happened during the sleep at very early stages of the disease development [28]. Other studies have developed wearable devices that measure gait parameters such as stride length, heel strike and toe off angle, toe clearance, etc. [18]. In their study, Johannes et al. used inertial sensors laterally strapped on both shoes. One problem regarding their approach is that it can cause discomfort to some patients because of the devices size. With the devices used in the Käveli project, discomfort is minimal since there shouldn't be any problems wearing a watch-like sensor and an insole. More studies regarding the gait cycle in PD were performed by Del Din et al. [29]. They also used triaxial accelerometers to study the asymmetry of the characteristics of the parkinsonian gait.

Overall it can be said that wearable devices have been widely used in the study of motor symptoms of Parkinson's disease because they seem to detect a large number of characteristics. Inertial sensors deserve special mention for their spread use and the amount of relevant data that has been collected from them.

3. MATERIALS AND METHODS

3.1 Study Material:

This thesis is done in cooperation with the Käveli Project, which is a research consortium of Tampere University (previously Tampere University of Technology), Satakunta Hospital District, Orionpharma Ltd, Suunto Ltd and Forciot Ltd, all based in Finland. Data was collected by the Käveli project during 2018 from a sample of 50 volunteer PD patients with early stage of the disease (no dyskinesia and state changes), plus 50 volunteer PD patients in the later stage of the disease (having dyskinesia and state changes), plus 50 volunteers who did not have Parkinson's disease. Background characteristics and stage of the Parkinson's disease has been evaluated in the hospital using a UPDRS questionnaires (Unified Parkinson's Disease Rating Scale; Finnish version) and a 20-step walking test [8].

Suunto Movesense ® gyroscope sensors were attached to the nondominant wrist and the participant wore a smart mobile phone with accelerometer and gyroscope sensors placed on the trunk. Suunto device had a sampling frequency of 52Hz and the cell phone signals were resampled at 100 Hz [Figure 1] [8]. Measuring ground forces on the feet was done via a Smart insole Forciot ® with a sampling frequency of 50 Hz [Figure 1]. The device replaces the shoe insole, avoiding as much discomfort as possible.



Figure 1. Devices used: Suunto Movesense sensor (top left), Forciot Smart insole (top right) and cell phone (bottom) [8]

Additionally, a 3-day motion screening in a free-living setting in which the subjects were wearing the phone during daily activities and marking down their PD medication intakes [8]. This part of the study was not used in this thesis. In total, 20-step walking tests measured at the clinic and a small subset of 8 subjects (4 patients and 4 controls) measured at the clinic with Suunto Movesense and Forciot Insole were used in this thesis. Python software was used for the data processing, plotting and analysis. The list of subjects used in this thesis is presented in Table 1.

Table 1. *Table containing all the subjects, first four with already diagnosed PD and the last four are controls.*

ID	Age	Weight (kg)	Height (cm)	Gender	UPDRS5
kav042	72	69	168	Male	4
kav096	47	54	162	Female	2.5
kav110	61	61	174	Male	1.5
kav112	67	64	155	Female	3
kav113	62	84	169	Female	0
kav114	44	95	186	Male	0
kav138	55	63	165	Female	0
kav175	71	70	180	Male	0

Both male and female performed the walking test. The age varied from 44 to 72. Weight varies from 54 to 95 kg, so the pressure data from the Forciot device was expected to vary greatly from one to another

UPDRS is a rating scale used to give a numeric value to the symptoms of PD. They don't only focus on the physical disorders, but also on cognitive impairment, hallucinations, depression or anxiety, for example. The numeric values vary from 0 (unilateral involvement) to 5 (wheelchair or bed bound unless aided) [9]. For this work, the overall score of modified UPDRS (test was MDS-UPDRS) was used.

3.2 Methods:

First step taken was to visualize the raw data and see how it is presented in the files. The Forciot data was stored in an array. In the first position there was the time data and in the second position there were different arrays as well with the signals from the insole sensors. The Suunto data was stored in an array of a length of 4. The first position was for the time and the other three were for the axes X, Y and Z in that order. Data was plotted like in Figure 2.

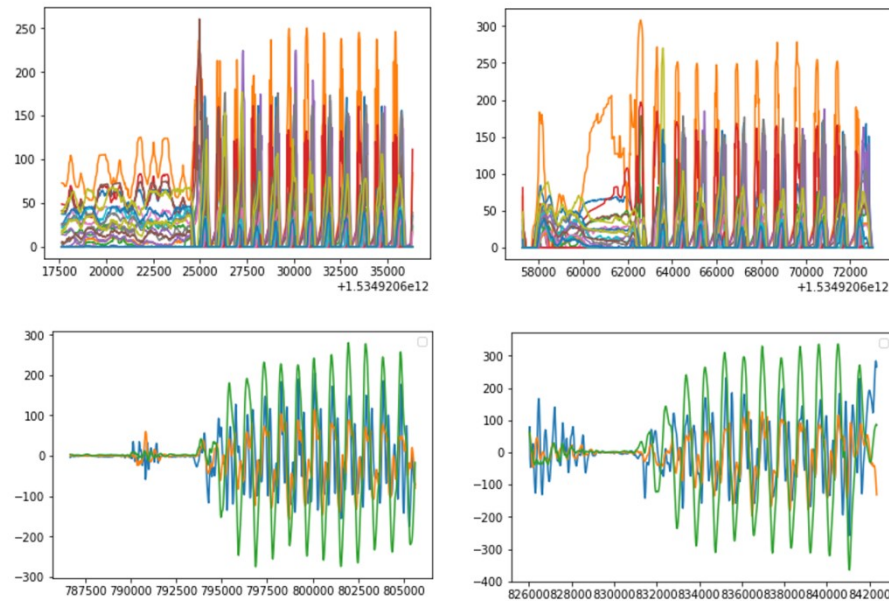


Figure 2. First visualization of the data of patient Kav113. Time was in Unix units. Forciot data on top plots the 23 sensors together. Suunto data on the bottom plots the angular velocity in the three axes. Both plots on the left represented the first test and the ones on the right the second one.

Time was converted from the Unix unit of time so 0 would be the start of the walking test. In order to do so in an iterative way and for easier access to the data for further application, the data from all 8 patients was stored in a matrix where all of them had their Forciot and Suunto data together. Then the conversion of the time vector was applied.

As it can be appreciated in all the plots, there is extra data at the beginning of each measurement that is not of any value. To solve this, the data had to be cut in order to only visualize the walking part of the test. In Figure 4, the difference between the cut and the raw data can be seen.

For easier visualization, a function was made to access all the data and plot either all the patients at the same time or the desired patient. The graphs would be shown not in their natural order (first the Forciot and then the Suunto), but on the test order, meaning that the Forciot and the Suunto samples from the first test would go first and the ones from the second test would go second as shown in Figure 5. Matching figures for all subjects are in Appendix A.

Subject Kav110. UPDRS 1.5. Test: 1

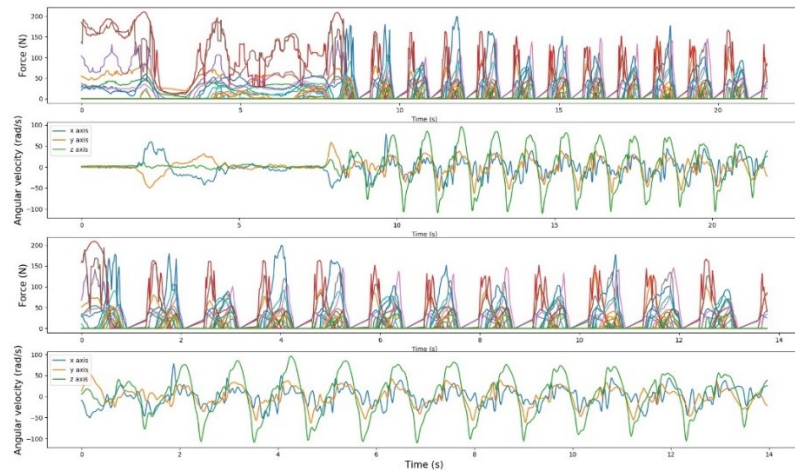


Figure 3. Difference between the raw (top) and cut (bottom) of the patient Kav110

Subject Kav113. UPDRS 0

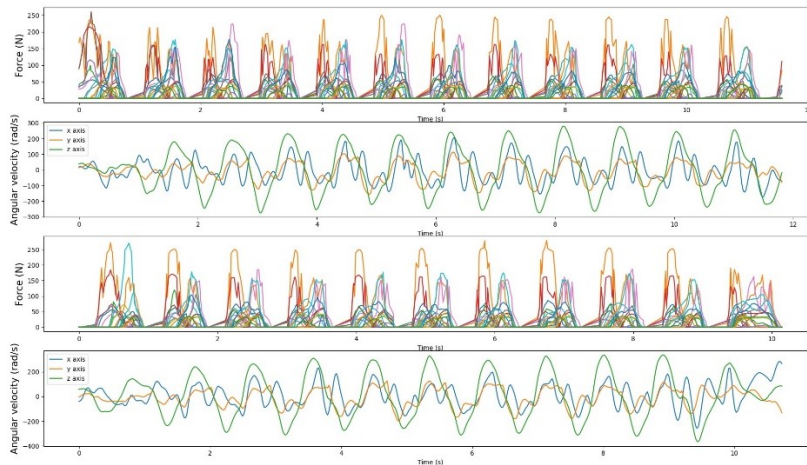


Figure 4. Example for subject Kav113 of how the data stored was represented. First and third figure come from Forciot device and second and forth from Suunto gyroscopes.

In order to be able to see the signal of each axis from the Suunto device separately for an easy study, the code added a new function that separated the three signals as shown in Figure 3.

Subject Kav113. UPDRS 0. Test: 1

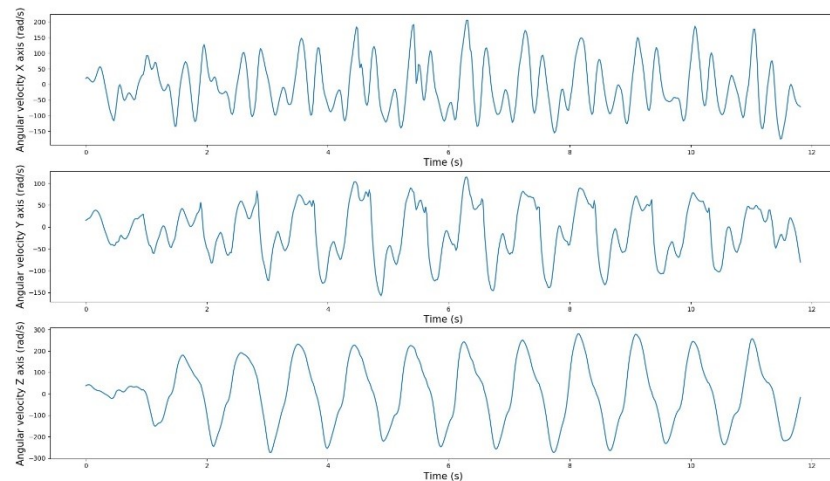


Figure 5. Plot of the Suunto data separately so the angular velocity can be seen in the three axes.

3.2.1 Forciot data analysis:

In order to visualize the Forciot signals better, they were plotted in a 2D matrix to be able to see how the force applied on each sensor changed. For that, first the position of each sensor on the insole was needed. Then, a grid was hand drawn to see which coordinates would the sensors take in the matrix. Since the hand drawn grid could deform the actual position, the sensors were represented then in a graph paper sheet top see if the image resampled the original as shown in Figure 6. Since it did, the position of each sensor was noted.

Then, to test the idea, the Forciot data of one patient was stored in one matrix of dimensions $22 \times 8 \times length$. 22×8 are the dimensions of the grid presented in Figure 6 and $length$ was the longest size of all the Forciot data. All the data was loaded in the written coordinates so each signal would be placed in the place of its corresponding insole sensor. Given the positive result, a list was created in order to have all the Forciot data placed in the sole matrix easily accessible and then saved. After that, the data was animated showed frame by frame and it can be seen how the pressure sensors of the Forciot device are activated during the stand phase of the gait cycle.

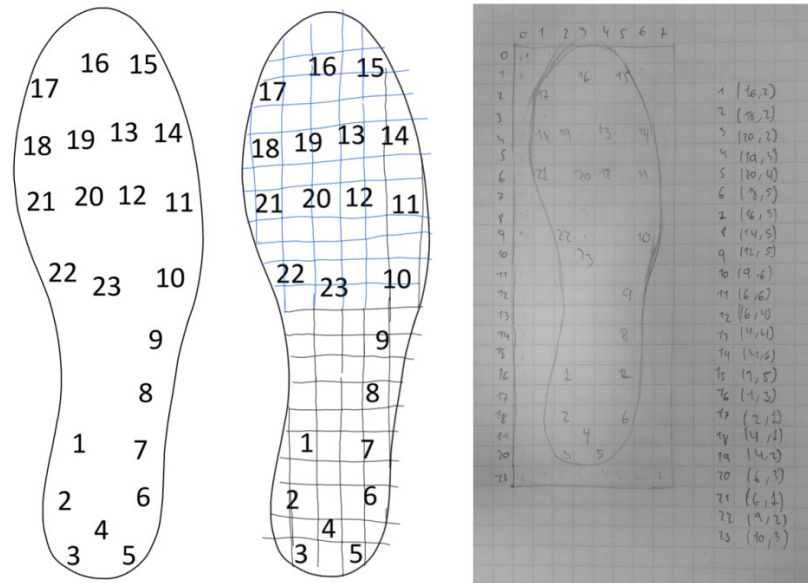


Figure 6. Original image of the pressure sensors (left), hand drawn grid over the original image (center) and the representation in a paper sheet (right).

The animation worked by doing a colormap based on a sample of the Forciot insole and then plot the rest of the samples “on top”. This was set using the first sample as default. Some data was cut when the insole sample had all the sensors signals to 0. As a result, the colormap was created with a colorbar around 0 like in Figure 7. Every sample after the first would be over the colorbar limit values; the result is a binary animation with a 0 value background and values over 0’1 in the sensors. To fix this, a function was created that would analyze every component of every sample of the test y of the patient x (inputs) and give as a result the sample in which the higher value was recorded (output). Then that sample would be the one used to create the first colormap and the rest would be animated over it. That way all the values of the sensors would be in between the values presented in the colorbar as shown in Figure 7.

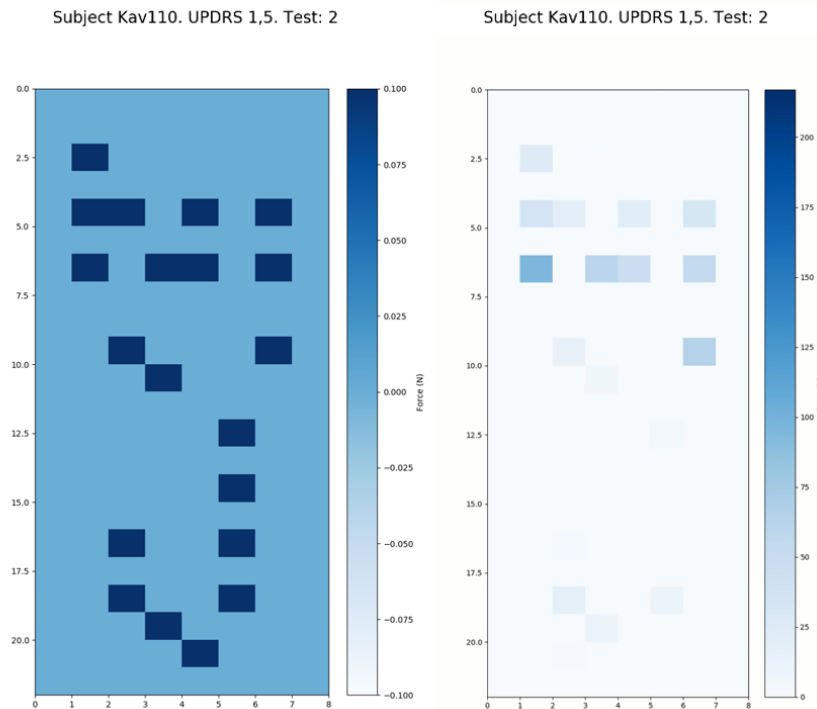


Figure 7. Example of a frame using the first colormap with a sample where all sensor signal is equal to zero giving as a result a binary image(left). The one on the corrected animation (right) has a range over 200 and the binary image only goes from -0.1 to 0.1.

In order to see the total input of the Forciot device, all the data from the 23 sensors was added for every measurement. As a result, the data is clearer and the differences between each patient can be seen, like in Figure 8. The steps were distinguishable and there was a clear difference between the swinging phase and the ground phase of the gait cycle. It could also be appreciated how there were peaks at the beginning and the end of the ground phase, which corresponded to the heel strike and the toe-off instants.

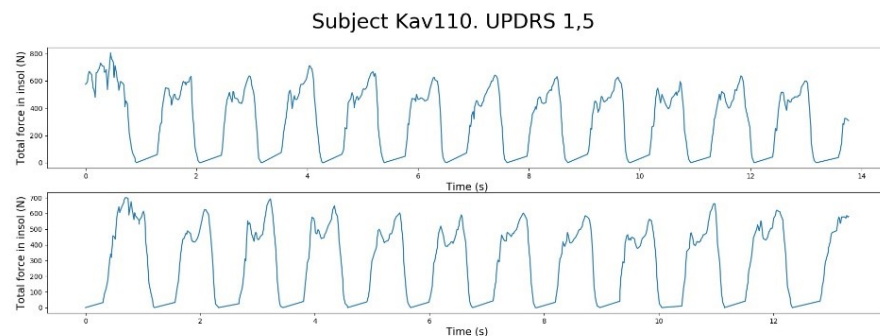


Figure 8. Total Forciot input of all the sensors in the insole.

After plotting the input signals, they were used to calculate the average time of a full gait cycle. For that, an algorithm was created in order to detect the beginning of every swinging phase (minimum value) taking into account that there was a minimum number of

samples required to get to the heel strike for every subject was just above 20 samples. Two consecutive points measured were considered the beginning and the end of the cycle.

When all sample numbers of the peak were saved, the time vector of each measurement was used to calculate the time it took to make one complete gait cycle and then the average for each test of each patient was calculated. It is also interesting to show the maximum input per step taken with the Forciot sensors. For that, the previous data was used so the steps could be separated and then from each step the highest value of the input was saved so then it could be averaged in every test. To see the area under each step they were separated and integrated each in their time intervals.

3.2.2 Suunto data analysis

Suunto gyroscopic sensor measured the angular velocity around the three axes like in Figure 10 in rad/s. It represents the velocity in which the rotation angle change in each axis, so when the sensor didn't detect any rotation, the output signal stayed 0.

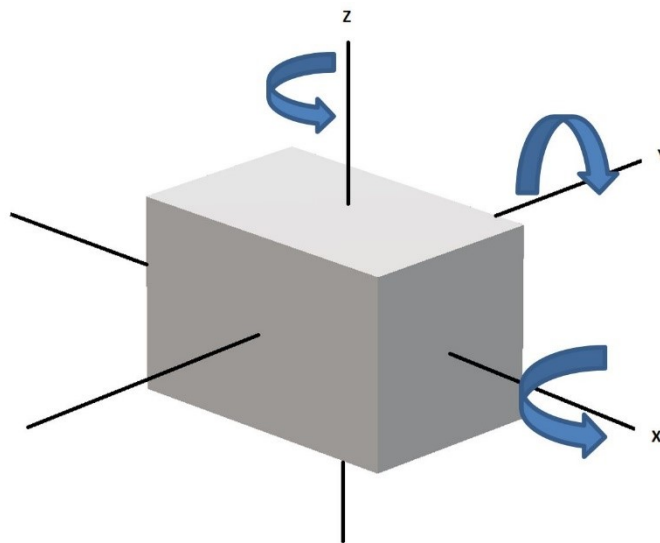


Figure 9. Representation of the rotation around the three axes.

It is useful to get the root mean square (RMS) of the angular velocity signal to get an average at which the movement of the hand happened [10]. In their study, Koop et al. used this value to measure bradykinesia[10]. FFT was performed for every subject and control and every axis separately, so differences in frequency of the signals could be seen in Figure 10.

Subject Kav042. UPDRS 4. Test: 1

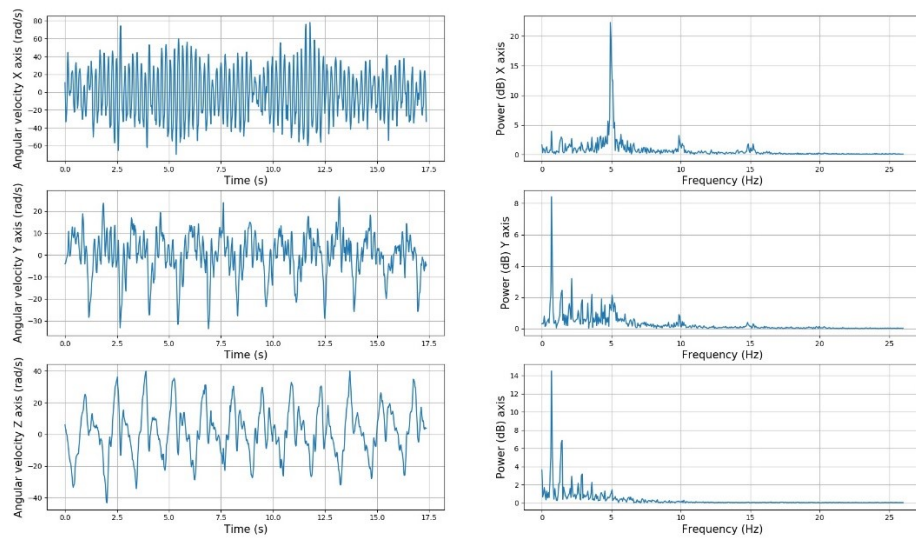


Figure 10. Data from Suunto represented on the left and the FFT on the right. X axis on top, Y axis on the center and Z axis on the bottom. Every FFT plot also has the RMS value of the signal.

The spectral entropy was calculated as well for every subject, every test and every axis direction. It would be expected that the higher the UPDRS level, the lower the entropy would be because of the tremor [11]. This was expected to happen because the tremor is usually regular, so the signal would be less random than the subjects with lower severity of the disease or the control. It has to be taken into account that all the tests were walking tests and thus, all of the signals oscillate in time. This can make the values lower. It should also be noticed that in their study, Rissanen et al. used acceleration signals and in this study the analyze signals are angular velocity [11]. These facts could potentially hinder the results.

There are studies of PD gait analysis using wearable sensors were researchers were able to distinguish events of FOG using the spectrogram of the signal (among other measurements) [20] [21]. Thus, spectrograms of the gyroscope signals were calculated in order to see if the frequency is consistent in time during the test or if there are some differences between the controls and the subjects affected with PD as presented in Figure 11.

Subject Kav110. UPDRS 1,5. Test: 1. Suunto Gyroscope Spectrogram

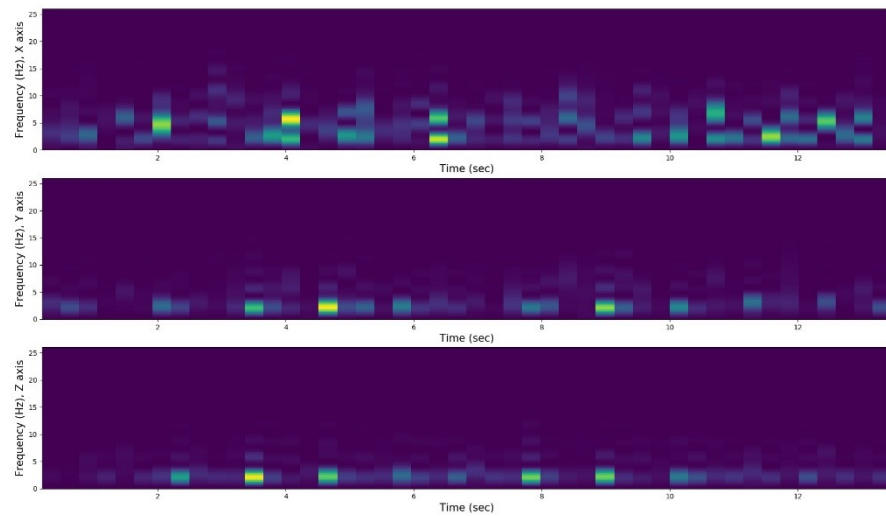


Figure 11. Spectrogram from the Suunto signal of subject Kav110. X axis on top, Y axis in the middle and Z axis in the bottom.

It also seemed relevant to see how the module of the three-dimensional vector was changing in time. This module was calculated taking into account that the three signals from the Suunto gyroscope represent at each sample the coordinates of a vector. FFT and spectrograms were also performed to the resulting signal and RMS and entropy were calculated as well. The ending result is shown in Figure 12.

Subject Kav110. UPDRS 1,5. Test: 1. Angular Velocity Vector Module

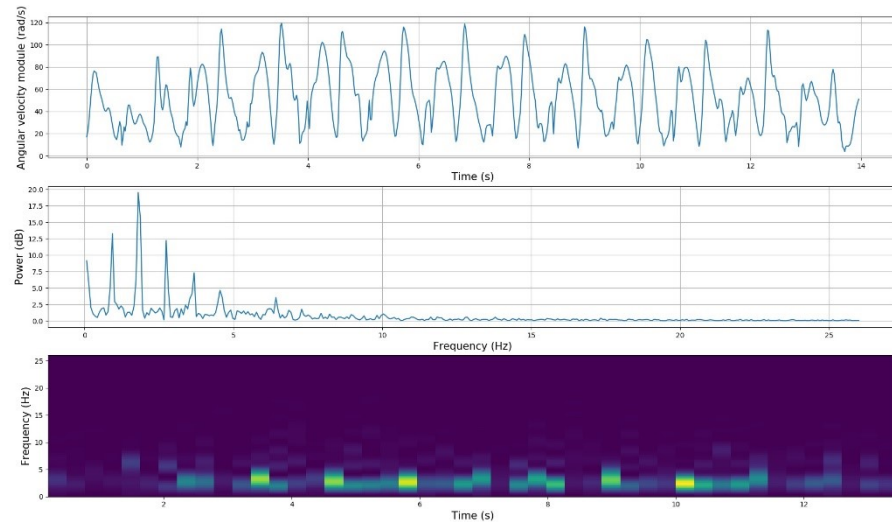


Figure 12. Variation of the module of the angular velocity vector in time of patient Kav110 (top), FFT of the signal (middle) and its spectrogram (bottom). Entropy and RMS values shown on the top graph.

4. RESULTS AND DISCUSSION

From a first look to the signals [Appendix A: Figures], it can be observed how the overall input in the pressure sensors of the Forciot device is lower for the Subjects with PD, being in a range up to 150-200 N while the controls showed ranges up to 250-300 N for individual sensors. Referring to the angular velocity data there is also a decrease in the range of values in the subjects suffering PD, being the lowest for subject Kav042 (UPDRS 4) with a range of -75 to 75 rad/s. It is also visible how the tremor affects the Suunto data in the subjects with PD. In the controls, the signals that appear during each gait cycle are very regular for the same patient. There are many differences between each other but that is just because of the different walking patterns that every person has, hence the need for the monitoring of every subject for a personalized treatment. PD subjects all show irregular patterns and, in some cases, indistinguishable cycles. This is a direct consequence of the reduction of the arm swing caused by the disease. Not only that, but for some signals it seemed that there is noise of high amplitude. This is the result of the tremor. It is less obvious in subject Kav110 (UPDRS 1.5) but it increases its intensity proportionally with the development of the disease, being most noticeable when the UPDRS value is 4 (subject Kav042).

The results are explained in depth in the following sections. They are separated by the type of signal, either force or angular velocity. The analysis of the Suunto data is also divided in four different sections. All the figures are presented in Appendix A.

4.1 Forciot Data Analysis

In the Forciot data analysis we can look at the total input data [Appendix A, Figures: Forciot total input data]. There is a clear difference between the ground phase and the swinging phase of the gait cycle, when the measured foot was on the air and thus, no force was applied to the sensor.

In the controls it can be clearly appreciated that there are two peaks in the ground phase that can be seen in Figure 13. The first one corresponds to the sensors place on the heel of the insole and they measured the heel strike and the beginning of the ground phase of the cycle. After that, there was a decrease in the total force in the midway and again an increase in the toe-off phase. This last increment was higher than the first peak and that is because there was an extra force that needed to be applied to propel the body and to perform the next step.

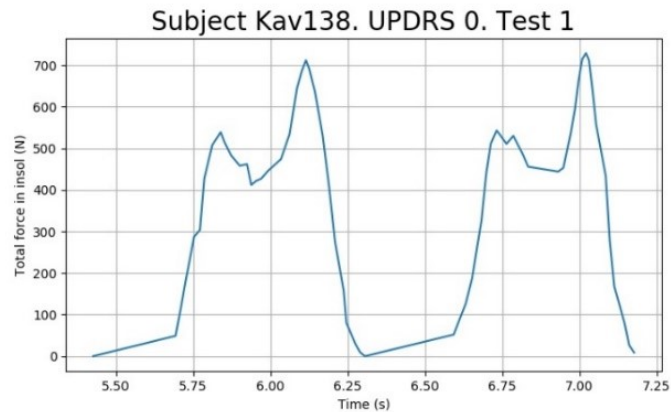


Figure 13. Total force signal from the Forciot insole of two full gait cycles of control subject Kav138. The two peaks corresponding to the heel strike take values of 536 and 540 N and the ones corresponding to the toe-off reach 708 and 722 N.

If the information of each sensor is taken separately from the same two gait cycles, like shown in Figure 14, it can be visualized how the activation of each one was at a different time of the ground phase. This corresponded to the shifting in the applied force on the foot, and therefore to the insole, during the swinging phase of the opposite foot in order to maintain balance and prepare the body to perform the next cycle. Each of the controls had a specific walking pattern and thus, it was reflected in the insole signal. Apart from these differences, all of them showed regularity on each test and all of them had the two peaks previously mentioned when analyzing the total input of the insole.

In Figure 14 it can be seen how the first sensors to receive pressure are the ones of the heel (2-6). In this particular case, the red signal is the highest, meaning that all most of the force is applied to the center of the heel (4). Then the signal coming from these sensors decrease and the force starts to spread through the rest of the sensors. It is visible how in this case, the most pressure is applied to the sensor 10 (light blue) and then it is transferred to sensors 12 and 20 (orange and light blue) and to finish to number 17 (pink). This is an example of how the force is differently applied through the foot in a healthy control, how there is an initial supination of the foot (sensor 10 activated) followed by a pronation (sensor 17 activated). This pattern is, again, specific for control subject Kav138.

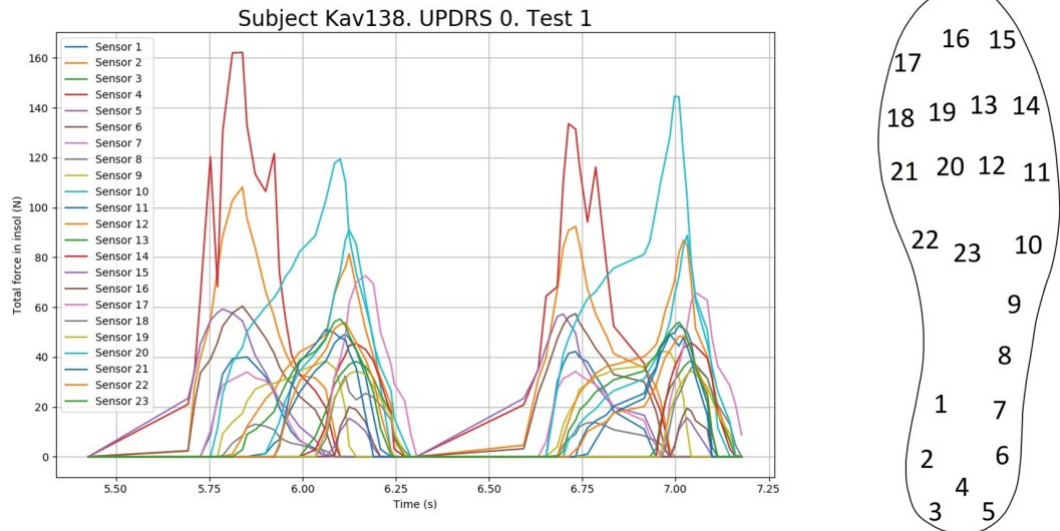


Figure 14. Force from each sensor of the Forciot insole of two full gait cycles of control subject Kav138 (left) and sensor placement on the insole (right).

When comparing the four PD subjects in Figure 15, it can be appreciated how there was an evolution. Subject Kav110 (UPDRS 1.5) showed some differences with the controls, both peaks in the ground phase can be seen in every gait cycle, first one (heel strike) reduced under 500 N in some cases but visible nonetheless. Subject Kav096 (UPDRS 2.5) also showed a decrease of the force applied in both peaks, most notably in the last one, just before the swinging phase, which is mostly equal to the first one and in some instances smaller, taking values between 450 and 500 N. Subject Kav112 (UPDRS 3) showed no distinguishable peaks in the first 3-4 steps of both tests and after, they became recognizable but smoothed. This might mean that the subject showed difficulty to perform correct steps at the beginning of the test. Subject Kav042 (UPDRS 4) showed none of the forms observed in the controls and individual peaks were not distinguishable. There was just an increase in the overall pressure applied to the insole and when the maximum force was reached, the signal simply decreased. The first assumption was that the heel-toe movement was not achieved and that the landing happened directly on the midfoot. The animation clearly showed a heel-toe movement which meant that even though it was present, the applied forces were very limited and the power in the toe-off phase was reduced.

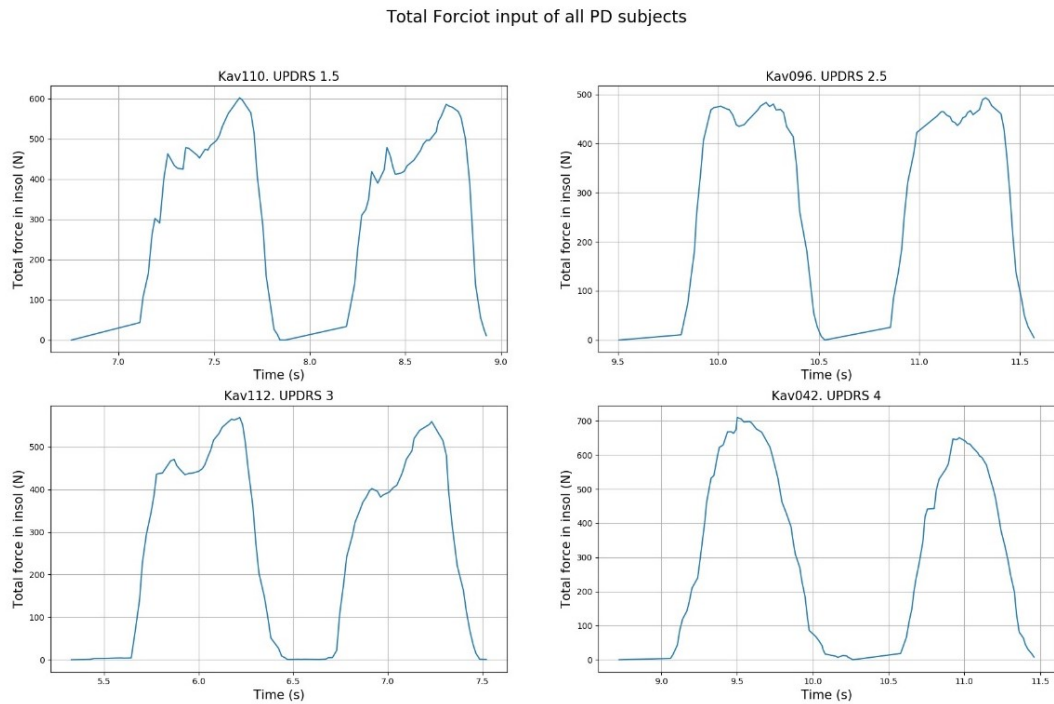


Figure 15. Total input from Forciot insole of all four subjects presenting PD disease. Kav110 (UPDRS 1.5) on the top left, Kav096 (UPDRS 2.5) top right, Kav112 (UPDRS 3) bottom left and Kav042 (UPDRS 4) bottom right.

The heel-toe patterns appeared to be different from the control subjects, as shown in Figure 16. Usually heel sensors experienced more force in the heel contact to the ground than the anterior sensors in the toe of phase. The exception was subject Kav096 (UPDRS 2.5), who showed very reduced heel force and higher pressure in the toe of phase. However, this force was reduced as well when compared to the controls. The overall progressive reduction in the toe off phase in all four subjects relates to the reduced ankle power generated in the gait caused by the reduced muscle activation consequence of PD.

This effect is best represented in subject Kav042 (UPDRS 4) data. When the steps had less “roll” in them, the weight was not correctly applied to the foot and it may have caused larger force at one time instances, shifting the gait pattern. Since there was no previous data of any of the subjects, there was no way of quantifying the variation suffered by the disease and how it affected the gait cycle in each specific case.

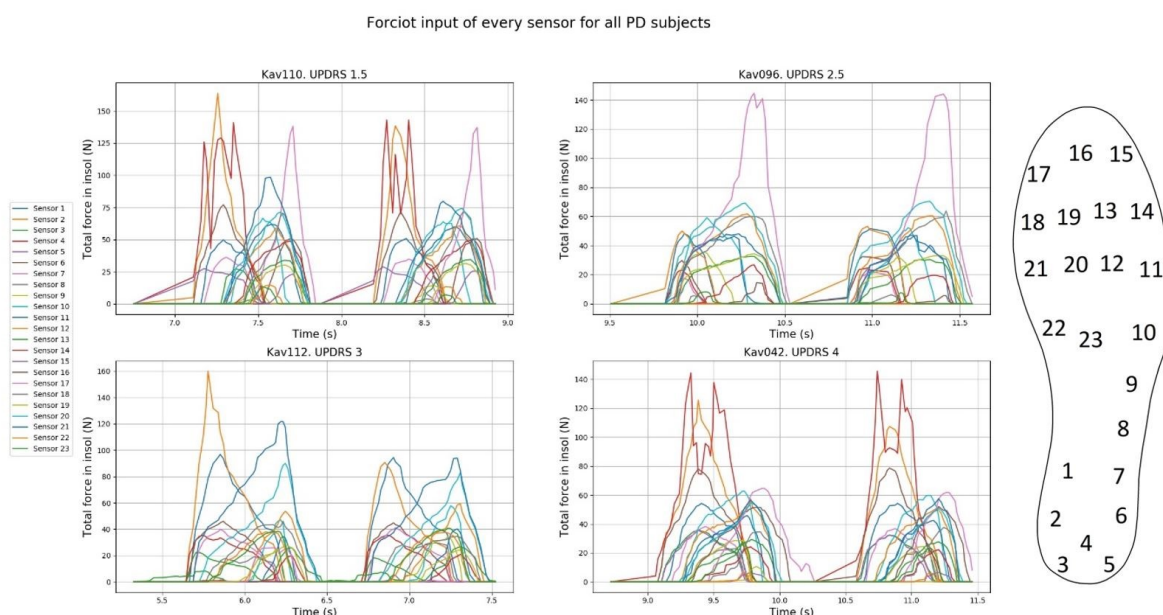


Figure 16. Force from each sensor of Forciot insole of all four subjects presenting PD disease. Kav110 (UPDRS 1.5) on the top left, Kav096 (UPDRS 2.5) top middle, Kav112 (UPDRS 3) bottom left, Kav042 (UPDRS 4) bottom middle and location of every sensor in the insole (left).

All these observable measurements from the pressure sensors are easily distinguishable in the animations so the physicians assessing the patients can see on first sight the level of pronation/supination and the weight distribution through the insole. A good assessment would require videos from different stages of the disease development, this would also include video recordings before and after the levodopa treatment to see visible changes.

The total input analysis that was explained in the methodology gave the results presented in Table 2. Since the data collected from the insole is highly influenced by the weight of the subject, the results were divided by the subject's weight so that it could give a result independent of it. There is no distinguishable pattern in the step time average and it seems that the different stages of PD don't affect the time step. There is only a relationship between the values of the different tests per patient, which suggest that the tests were correctly performed so there were no significant differences in between the them. The maximum value recorded in the insole didn't show any correlation with the stage of the disease. Same seemed to happen in the area under the graph, average of the integrated input.

Table 2. *Table containing the average step time, average max input and the average integral per step. The number (Forciot 1-2) refers to the test number.*

Subject	Test	AVG step time (s)	AVG max input (N)	AVG max input (N/Kg)	AVG integrated input (N)	AVG integrated input (N/Kg)
kav110	Forciot 1	1.11	636.49	10.43	332.61	5.45
	Forciot 2	1.11	619.42	10.15	300.12	4.92
kav096	Forciot 1	1.07	522.04	9.67	289.99	5.37
	Forciot 2	1.02	506.18	9.37	272.34	5.04
kav112	Forciot 1	1.07	556.94	8.70	305.66	4.78
	Forciot 2	1.08	581.69	9.09	395.81	6.18
kav042	Forciot 1	1.43	678.24	9.83	417.16	6.05
kav113	Forciot 1	0.95	894.02	10.64	419.37	4.99
	Forciot 2	0.90	829.02	9.87	358.70	4.27
kav114	Forciot 1	1.12	1113.10	11.72	565.84	5.96
	Forciot 2	1.14	1164.98	12.26	589.88	6.21
kav138	Forciot 1	0.90	730.78	11.60	261.15	4.15
	Forciot 2	0.90	708.53	11.25	256.30	4.07
kav175	Forciot 1	1.13	764.18	10.92	376.67	5.38
	Forciot 2	1.12	774.27	11.06	388.30	5.55

Observing the results in the averaged maximum input, there is a tendency to get lower values, the higher the PD stage. This is due to the reduction in the strength applied against the ground in PD patients. To establish patterns, a statistical analysis with bigger sample number would be needed. All the controls got higher values in both of their tests compared with PD subjects except for test number two of subject Kav113, which was lower than both subject Kav110 (UPDRS 1.5) tests. Surprisingly, subject Kav042 (UPDRS 4) got a higher result than subjects Kav096 and Kav112 (UPDRS 2.5 and 3 respectively). There is no relationship between the area under the graph. All the data seems consistent between both tests except for subject Kav112. It can be inferred that the subject didn't walk the same way in both tests.

The lack of relation between the results portrayed in Table 2 and PD stage may be due to the fact that the sample size is small and the tests were performed in different subjects with individual walking patterns. It has been previously explained how the gait is affected by PD. Using the insole during longer periods of time would provide more accurate data and more personalized analysis, since each person has a different gait. It would be interesting to see the healthy step time of each subject and see how the disease affected the speed of it and the frequency of the steps. Longer period of measurement would also provide a good input in the variation of the power applied against the floor, on the insole in this case.

4.2 Suunto Data Analysis

The Suunto gyroscopic sensor was placed on the subject's wrists and thus, the angular velocity measured around the three axes corresponds to the arm swing movements performed in the gait cycle. These movements are caused by the shoulder flexion, moving the arm forward, and extension, pulling the arm backwards. Most of the subjects, angular velocity (AV) around the X axis was messy, with the exception of control subject Kav114, who showed clear patterns that repeated evenly through both tests. All control subjects showed similar patterns around the Y axis except subject Kav113, who showed a different one, but consistent through both tests, reflecting his unique walking pattern. Controls Kav113 and Kav138 showed similar patterns around Z axis, where there are basically straight lines in positive and negative directions with peaks in both extremes (sometimes smoothed in the positive direction). Subjects Kav114 and Kav175 (also controls) also had similar patterns around Z axis, but differing from the other two controls. They showed a first peak in the positive direction and then, there was a stop in the negative oscillation where the signal either flattened around 0 or decreased its gradient for a moment. All positive gradients were straight and showed no disturbances. These results showed that the healthy gait cycle is not symmetric in concern with the swinging of the arms to counterbalance the body movements, meaning that the shoulder flexion and extension movements do not follow the same path during the gait cycle. Example of three complete cycles are shown in Figure 17. Rotation stayed minimal around X axis when both Y and Z rotations were negative and peaked when they were positive.

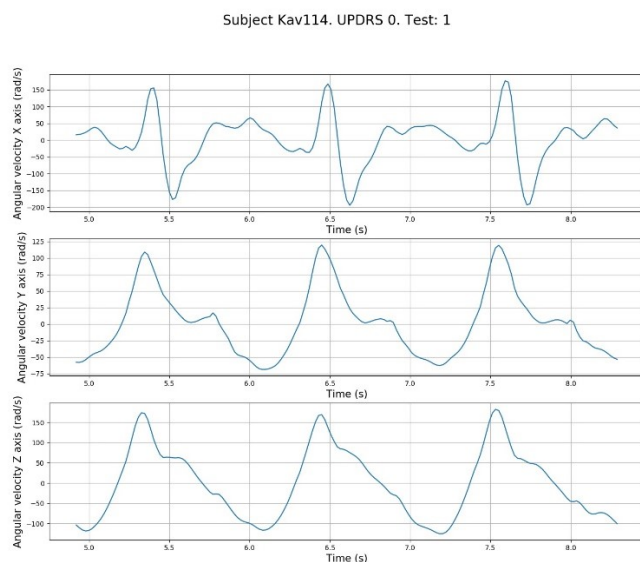


Figure 17. *Three complete gait cycles from subject Kav114. AV measured around X (top), Y (center) and Z (bottom) axes.*

All the data from the subjects with PD showed signs of tremor. In subject Kav110 (UPDRS 1.5), tremors (even though of low amplitude) were especially visible in the X axis, where a cyclic pattern was barely visible. In the other two directions, tremors were not distinguishable and the cyclic patterns were distorted, especially around Y axis. Maximum values were achieved around the Z axis and reached the 100 rad/s, lower than all the controls. Amplitude of the signal around both X and Y axes was reduced as well. Thus, the effects of bradykinesia and rigidity, even though they were mild, were noticeable from the first stages of the disease.

Subject Kav096 (UPDRS 2.5) showed signs of high amplitude tremor visible in the three axes. The only distinguishable gait cycle appeared on the Y axis. The lack of distinguishable patterns and the diminished amplitude in the Y axis was a sign of a further development of PD and the effects of rigidity, bradykinesia and tremor in a higher degree.

Subject Kav112 (UPDRS 3) again showed even higher degree of tremor (and of higher amplitude) and no oscillations in both X and Y axes. Z axis was not affected as much by the tremor but the gait cycles were irregular and showed high changes in the direction of the angular velocity happened within them.

Subject Kav042 (UPDRS 4) didn't show any signs of oscillation whatsoever in the X axis measurement, only a high amplitude 5 Hz vibration caused by the tremor. Both Y and Z axes showed small oscillations and even repetitive patterns. While the signal around Y axis seemed messy and the only discernible patterns were peaks in the negative direction, the cycles around Z axis resembled the patterns that controls Kav114 and Kav175 showed, only reduced in amplitude (100-200 rad/s in control against 40 for subject Kav042). This was due to bradykinesia and rigidity and also showed higher frequency noise due to the tremor. The uncommon results from this subject could be due to the fact that he presented hemiplegia had great difficulties walking so he needed a rollator to move.

4.2.1 Frequency domain.

When performing the FFT to the signals, all controls showed a high peak in the frequencies around 1 Hz. This is the result of the arm swing during the gait cycle, that makes around one full swing cycle per second. This peak was more prominent in the Z axis in all the controls and was reduced around the X axis. In control Kav138 it wasn't not noticeable. All X axis measurements showed peaks at higher frequencies which implied that the movements in this axis were not influenced that much from the arm swing itself but from the different rotations that took place in different directions within the same cycle. These extra peaks are different per control subject but consistent in the two tests

taken, meaning that they are related to the specific way of walking that each one of them had.

For subject Kav110, the main peak at 1 Hz was maintained in the three axes, reaching its highest amplitude in the Z axis like in the controls but there was a decrease in power due to the effects of rigidity and bradykinesia. The tremor, as explained in the previous section, was mostly noticeable in the X axis but, since it had a really low amplitude due to the early stage of PD, there are several smaller peaks at higher frequencies.

Subject Kav096 had higher frequency disturbance that corresponded to the tremor and higher rigidity level, which were more noticeable than the previous subject since he was in a further stage of the disease. The only axis that had distinguishable cycles was the Y axis and, thus, there was a higher peak at 1 Hz. In the other two axes, this peak was very reduced and others appeared at higher frequencies due to irregular movements during the gait cycle. There was still no peak in a higher frequency that can be distinguished as the frequency of the tremor, but rather a combination of the mechanical impairments caused by the disease.

Subject Kav112 had a further development of the disease and the effects of Parkinsonism were reflected in the frequency domain. There was a very reduced peak at 1 Hz characteristic of the healthy gait and there was a higher peak at 2 Hz that could be measured in all axes and both tests. This was a direct effect of the reduced arm swing caused by the rigidity (lower 1 Hz) and smaller faster compensatory movements (2 Hz). Tremor was mainly measured in X and Y axes and here there was a clear peak in which it could be measured, better seen in Y axis, reflecting the regularity of the movement. Tremor showed at a frequency of 5.5 Hz as seen in Figure 18.

Kav042 had the highest mark in the UPDRS of the four PD subjects. Surprisingly the tremor was almost only felt in the X axis where practically no other component of the signal was recorded. This may be caused by the aid of the rollator mentioned before that was needed to walk. In the FFT, there was only one peak in the X axis corresponding to the tremor at 5 Hz. In the other two axes, the peak at 1 Hz reappeared but with a very low power due to the reduced movements of the subject. The small shift in the tremor peak compared with subject Kav112 infers that, even though the tremor was regular in general terms for PD, the frequency at which it occurs is slightly different to each patient. It can also mean that there is an effect in the tremor frequency related to the different stages of PD, but since there was no previous data from these subjects it couldn't be evaluated statistically if the tremor frequency was altered in the development of the disease.

Subject Kav112. UPDRS 3. Test: 1

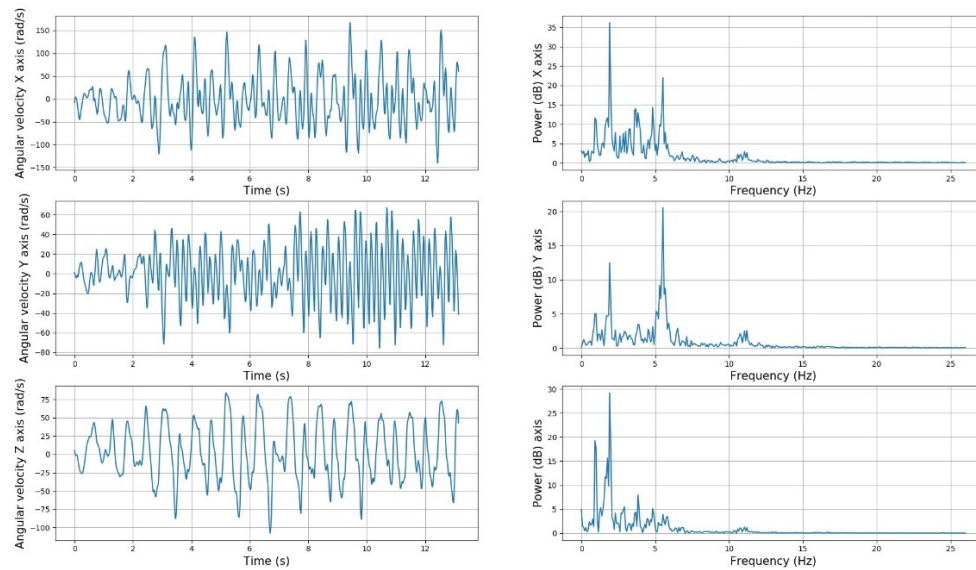


Figure 18. Time (left) and frequency (right) analysis of angular velocity data around the three axes from subject Kav112.

4.2.2 Time-Frequency.

The spectrograms of the data were performed to see the variation in frequency of each axis data during the tests. All the controls showed similar patterns, high power at low frequencies spread evenly through the whole test. The regularity of the signal showed the components of the healthy gait cycle were the same on each step. For control Kav175 the Spectrogram around X axis was more disturbed but all the power of the signal was maintained at lower frequencies, all under 5 Hz.

For subject Kav110 (UPDRS 1.5) signal power was spread through higher frequencies through the test in the X axis, from seconds 7 to 10, there was a general drop in power of the signal. The signals in the other two axes were very similar to the controls, cyclic lower frequency peaks with reduced power evenly distributed throughout the test.

Subject Kav096 (UPDRS 2.5) got more irregular data in both tests. The messiest signal was shown in the X axis where there was no clear cyclic pattern. The power from the signal was spread through higher frequencies and the lower frequencies were reduced in power. Signals around the Y axis were also messier than subject Kav110 and no patterns were recognizable but the power at lower frequencies was still maintained. Z axis signals showed lower power with some high power at low frequencies eventually but no discernible cyclic patterns.

Subject Kav112 (UPDRS 3), showed no high power in the signal at high frequencies but there was a distinguishable high-power line that remains constant during the whole test

at 5Hz, characteristic of the tremor. This tremor line was more distinguishable in the Y axis, as it can be appreciated in Figure 19. Here, the peak at this frequency was located in the FFT analysis from the previous section. Z axis showed consistent power levels at lower frequencies in both tests but no patterns were distinguishable.

Subject Kav112. UPDRS 3. Test: 1. Suunto Gyroscope Spectrogram

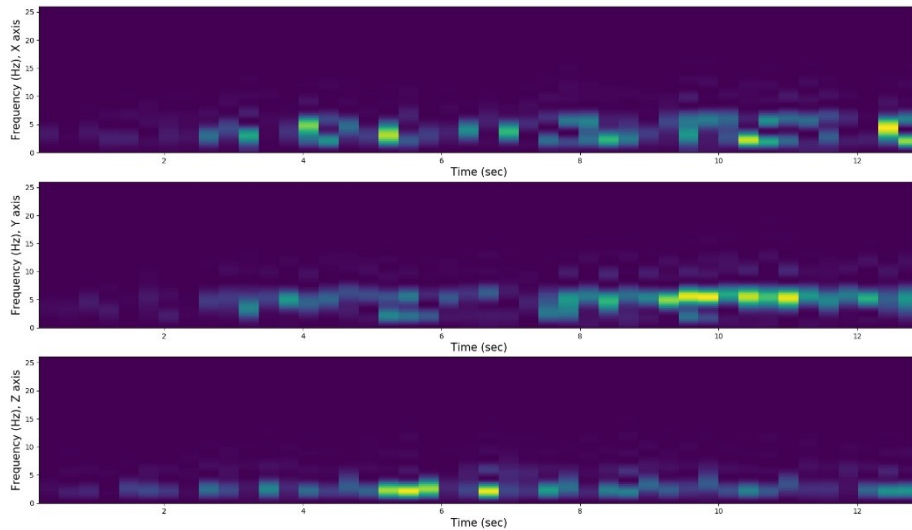


Figure 19. Spectrogram of the angular velocity signal from subject Kav112.

Subject Kav042 (UPDRS 4) had a prominent feature in the X axis, there was a constant line through the test at around 5 Hz that reflected the effects of the tremor, which didn't show equally in the three axes. These frequencies appeared again in the Y axis but of smaller amplitude because the original signal wasn't affected as much by the PD feature. In the Z axis, there was as a clear cyclic pattern, that, while it had less power than the other signals, it was clear.

The walking tests analysis using the spectrogram proved valid to visualize the effects of the tremor (power of the signal around 5 Hz) and the bradykinesia (Power of the signal at 1-2 Hz). It also was useful to distinguish clear cyclic patterns that repeated per gait cycle that can be used to detect alterations on the walking patterns in frequency and time. No events of freezing of gait were detected in the spectrograms.

4.2.3 RMS and Entropy.

As mentioned in the methodology, RMS value has been used to quantitatively study bradykinesia in people with the disease [10]. In this study the RMS was obtained to see if it could also assess this feature while walking and to study if there was a pattern in the different stages or the disease. The results obtained are presented in table 3.

Table 3. RMS values of every patients Suunto data. The number (Suunto 1-2) refers to the test number.

Subject	Test	X axis	Y axis	Z axis
kav110	Suunto1	21.500	22.341	49.406
	Suunto2	21.994	22.533	44.828
kav096	Suunto1	34.148	21.340	18.469
	Suunto2	41.647	20.466	16.827
kav112	Suunto1	52.250	27.407	38.851
	Suunto2	61.528	33.172	38.454
kav042	Suunto1	28.053	9.921	15.722
kav113	Suunto1	79.701	61.014	149.988
	Suunto2	98.440	73.106	182.761
kav114	Suunto1	80.032	49.486	83.200
	Suunto2	70.020	40.135	66.937
kav138	Suunto1	53.144	86.657	127.727
	Suunto2	55.710	88.633	122.249
kav175	Suunto1	30.344	51.179	63.625
	Suunto2	37.552	61.140	82.480

There was no apartment relationship between the RMS value in the X axis signal with the stage of PD. It seemed that the higher the UPDRS level, the higher the RMS value got, but it dropped for subject Kav042. The controls showed a long range of values from 98.440 to 30.344. Around the Y axis, the RMS was always lower on the subjects with PD than the controls. Values ranged from 40.135 to 88.633 while the lowest value obtained by the study subjects was 9.921 from Kav042 and the highest was 33.172 by Kav112 (UPDRS 3). Again, apart from the range of values, which were always lower for the PD subjects, there was no relationship with the stage of the disease.

The only values that showed some relationship were the ones in the Z axis, where the arm swing was reflected. The Values in all the controls were notably higher than the ones for subjects with PD. Except of subject Kav112 (UPDRS 3), the RMS Seemed to get lower the higher the PD stage.

The entropy of the signals was expected to get lower the higher the higher the stage of PD [11] This is due to the reduction in the amplitude of movements due to bradykinesia and the regular nature of the tremor, meaning that the movements in the controls would be more irregular and random. The results are shown in Table 4.

Table 4. Spectral entropy of every patient's Suunto data. The number (Suunto 1-2) refers to the test number.

Subject	Test	X axis	Y axis	Z axis
kav110	Suunto1	0.564	0.408	0.297
	Suunto2	0.561	0.437	0.329
kav096	Suunto1	0.790	0.560	0.723
	Suunto2	0.746	0.508	0.705
kav112	Suunto1	0.599	0.537	0.484
	Suunto2	0.563	0.493	0.472
kav042	Suunto1	0.399	0.591	0.472
kav113	Suunto1	0.491	0.382	0.233
	Suunto2	0.502	0.388	0.226
kav114	Suunto1	0.578	0.368	0.300
	Suunto2	0.552	0.379	0.310
kav138	Suunto1	0.573	0.275	0.216
	Suunto2	0.515	0.272	0.220
kav175	Suunto1	0.589	0.263	0.331
	Suunto2	0.529	0.259	0.328

There was no apparent relationship between the UPDRS value and the normalized entropy around the X and Z axis, the range of values was very similar, being the highest in subject Kav096 (UPDRS 2,5). Around the Y axis, all controls scored lower than PD subjects. The higher the PD stage, the higher the entropy every subject scored (again higher scored by subject Kav096). The main score for PD subjects was 0.60, 0.50 and 0.50 for X, Y and Z axes respectively while controls scored a mean of 0.54, 0.33 and 0.26.

The obtained values seemed to contradict the previous prediction and the study made by Rissanen et al. [11]. It has to be taken into account that their study used acceleration data and this one used angular velocity data. On the other hand, this study was based on walking tests. This means that, during the gait cycle, the healthy arm movement followed a regular pattern, since the swinging was not altered by other movement dysfunction, thus, the regularity of the movements done by the controls lowered their scored of normalized entropy. Reduction of the arm swing and the appearance of the tremor should lower the entropy per se but, since there were other components of the signals due to the irregularity of their gait cycle, the overall entropy increased.

4.2.4 Vector module.

Treating the Suunto data at each sample as the three space coordinates (X, Y and Z) of the angular velocity vector, the same analysis on its module ($\sqrt{X^2 + Y^2 + Z^2}$) seemed interesting. All control subjects showed distinctive cyclic patterns that stayed constant during both tests, which proved that the individual way of walking was reflected in the recorded signal. The values for the controls ranged from 160 to 400 rad/s

All the controls showed high power of the FFT at 2 Hz, as seen in Figure 20. Control subject Kav114 also showed peaks at 1 Hz and Kav175 at 1 and 3 Hz of lower amplitude. The peaks in the FFT were at the double of the frequencies that they were when the signal corresponded to the three axes instead of the module. All the control spectrograms showed regular patterns in the lower frequencies (around 2 Hz) during the whole test. Control subjects Kav175 and Kav114 showed intermittent patterns that reflect the arm swing movement.

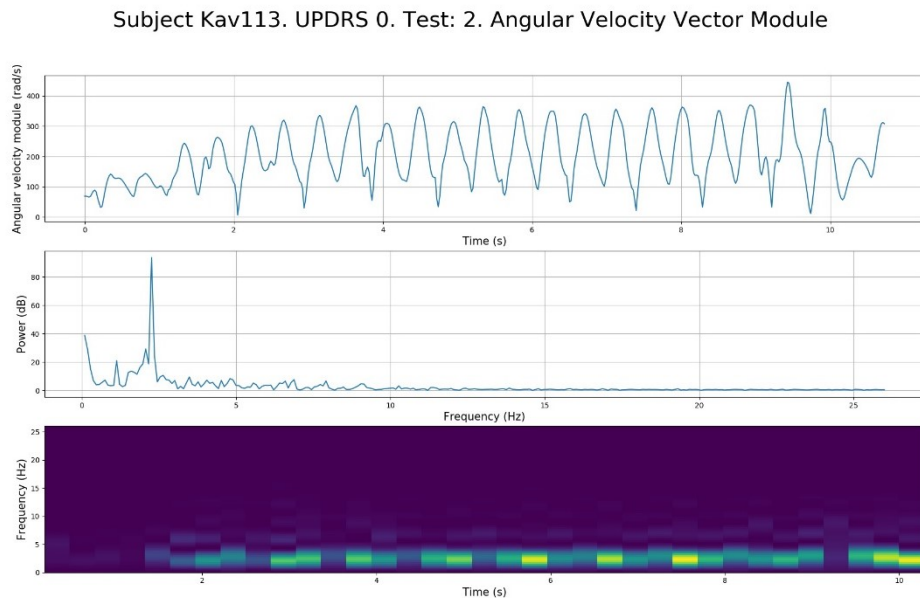


Figure 20. *Analysis of the angular velocity vector module for control subject Kav113.*

Kav110 (UPDRS 1.5) showed similar patterns than controls Kav114 and Kav175 but reduced in amplitude, reaching maximum values at 120 rad/s. The effects of the tremors were reduced or not visible in the signal of the module. The FFT of the signal is highly similar to the ones of the previous mentioned controls, with the highest peaks at 2 Hz and no higher frequency peaks from the tremor. The spectrogram didn't show any components in higher frequencies that would correspond to the effects of the tremor and no other remarkable modifications from the controls.

Subject Kav096 (UPDRS 2.5) had a messier signal, with no discernible patterns or peaks, the maximum value of the module reached 140 rad/s but the signal was completely distorted. The spectral power didn't show any peaks at any frequency and the spectrograms had instances with higher frequencies than what usually were presented in the rest of the signals but of lower frequencies. It has to be assumed that the performance of the vector module for the Suunto output of this subject completely altered the resulting signal making no observable features.

Subject Kav112 (UPDRS 3), Signal was greatly altered from the controls. There is no discernible patterns and the maximum value obtained by the module was 175 rad/s. The signal's FFT, showed a peak at 2.5 Hz and other peaks at higher frequencies (7 and 11 Hz) but of lower power. The spectrogram showed higher frequency components of lower power. Although the test reflected the effects of the tremor, but didn't seem as constant as it was reflected in the signal divided in the three axes.

Subject Kav042 (UPDRS 4) had notably the most affected signal. The effects of the tremor were obvious and there were no recognizable patterns. The highest value obtained by the vector module was 80 rad/s. The FFT of the signal was quite explanatory, there was a lower power peak at 2Hz and a higher power peak at 10 Hz. These power peaks were reflected in the spectrogram and maintained during the whole test, being more intense the ones at 10 Hz. If taken into account the first assumption that the FFT of the vector module gave peaks at the double value of frequency that the ones obtained in the previous sections, these peaks corresponded to the walking cyclic pattern (2 Hz) and the effects of the tremor (10 Hz). The RMS and the Entropy of the signals were again calculated and the results are presented in Table 5.

Table 5. *Table containing the RMS and entropy values for the module of the angular velocity vector for every test.*

Subject	Test	RMS	Entropy
kav110	Suunto1	58.330	0.514
	Suunto2	54.783	0.538
kav096	Suunto1	44.302	0.884
	Suunto2	49.361	0.867
kav112	Suunto1	70.644	0.740
	Suunto2	79.780	0.724
kav042	Suunto1	33.654	0.786
kav113	Suunto1	180.476	0.347
	Suunto2	220.083	0.331
kav114	Suunto1	125.604	0.538
	Suunto2	104.853	0.563
kav138	Suunto1	163.242	0.391
	Suunto2	160.948	0.418
kav175	Suunto1	87.111	0.487
	Suunto2	109.322	0.482

The first notable thing was that the RMS values of the controls were higher than the ones presented in subjects with PD, with the exception of test one from control Kav175, whose RMS value was 87.111. There was a clear tendency to decrease the RMS value when the UPDRS got higher, from a score of 58.330 from subject Kav110 (UPDRS 1.5) to 33.654 from subject Kav042 (UPDRS 4). There is an exception with subject Kav112 (UPDRS 3) who obtained values over 70.

Once again, the assumption made by Rissanen et al. [11] was not observed in these values since all PD subjects obtained a higher entropy than the controls. There was no apparent relation between the stage of the disease and the level of entropy since the lowest values were obtained by subject Kav110 (UPDRS 1.5) and the highest ones by subject Kav096 (UPDRS 2.5).

Overall the calculation of the angular velocity vector module only gave some results regarding the visualization of patterns while walking and how the tremor and the bradykinesia affected the signals. No optimal measurement of the tremor was achieved, with the exception of subject Kav042, since most of the PD signals turn out messier and both their FFT and spectrogram were more difficult to interpret. The entropy value of the signals seemed always higher in the PD subjects but no correlation with the level of the disease was detected. There was a clear pattern regarding the RMS value of the signals, which got lower the higher the UPDRS value. This is because, since the movements of people with parkinsonism are reduced in amplitude and affected by higher frequency tremors, that relates in the signal as lower amplitude than the ones generated from the natural movement. The overall signal suffered a reduction in its variation during the gait cycle, the opposite than the controls signals which reflected higher amplitude of movements and, thus, a greater variation.

5. CONCLUSIONS

There has been already a number of studies assessing the detection or diagnosis of Parkinson's Disease using wearable devices [17]-[18] [20]-[21] [24]-[29]. This technology allows a new form of evaluation of the features that encompass the disease. The main problem regarding the assessment of the disease is the lack of daily data that can be provided to the healthcare professionals since the tests regarding the evaluation of the disease are performed in long time intervals. This information is usually provided by family members, professional personnel taking care of him/her or the patient themselves, which does not provide an objective input on the stage of the disease. Another lack of information comes from the specific response to levodopa dosage. It should be individually measured since it can vary from patient to patient, so that the treatment can be effectively applied. The use of long-term wearable devices provides a solution to this problem since they can measure specific parameters during extended periods of time, detecting how PD affects the signals measured by the devices. The interpretation of these data by the healthcare professionals is key to properly assess the stage of the disease in which patients are and provide a proper treatment.

The use of the Forciot insole and the Suunto gyroscopic devices provides a good solution to the problem. These devices are worn with minimally invasiveness or discomfort. Forciot insole provides a good visualization of the walking patterns of the wearer and gives a result of the distribution of force during the phases of the human gait cycle. The study showed the reduction of the force applied against the ground by the subjects with PD, especially during the toe-off phase, at the end of the cycle.

Suunto gyroscopes were especially useful in the visualization of walking patterns in the arm swing and the effects of bradykinesia and tremor on the signals. Frequency analysis were useful to assess the frequency components of the signals and more specifically to the tremor detection. Spectrogram analysis was also useful detecting the tremor in periods of time. This would be especially useful in long term signals where the severity of the movement disorders fluctuates from one day to another. RMS values only proved quality results regarding the stage of the disease when performed on the module of the angular velocity vector rather than the signals separated by each axis. Normalized entropy values didn't give any input on the UPDRS level of the subjects, thus proving to be an ineffective measurement with gyroscopic signals of walking tests.

The application of wearable devices to visualize the motor features of PD provide a promising solution to the monitoring of people suffering the disease. The low cost of this kind of technology makes it more available to the public use and it makes possible to perform population-based epidemiological researches that other technologies do not achieve such as medical imaging methods.

Since the data used in this study was obtained from a 20-step walking test performed at the clinic for a small subset of eight people, there was no way to compare the effect of PD during different stages of the disease for the same patient. This could be used to assess specific alterations in the movement of each patient individually which would be a used to distinguish the specific patterns of a subject and compare it to the effects of parkinsonism.

The use of the Forciot smart insole and the Suunto Movesense gyroscopic sensor proved to be useful distinguishing some motor features of parkinsonism during different stages of the disease and proved to be a possible solution to the home monitoring problem reducing as much as possible the discomfort that could be generated. There should be further studies in order to find an optimal solution and the most efficient methods that could be used with these wearable devices.

REFERENCES

- [1] Polymeropoulos MH, Lavedan C, Leroy E, Ide SE, Dehejia A, Dutra A, et al. Mutation in the α -synuclein gene identified in families with Parkinson's disease. *science*. 1997;276(5321):2045-7.
- [2] De Lau LM, Breteler MM. Epidemiology of Parkinson's disease. *The Lancet Neurology*. 2006;5(6):525-35.
- [3] Postuma, R., Berg, D., Stern, M., Poewe, W., Olanow, C., Oertel, W., Obeso, J., Marek, K., Litvan, I., Lang, A., Halliday, G., Goetz, C., Gasser, T., Dubois, B., Chan, P., Bloem, B., Adler, C. and Deuschl, G. (2015). MDS clinical diagnostic criteria for Parkinson's disease. *Movement Disorders*, 30(12), pp.1591-1601.
- [4] Jankovic J. Parkinson's disease: clinical features and diagnosis. *Journal of neurology, neurosurgery & psychiatry*. 2008;79(4):368-76.
- [5] Berardelli A, Rothwell JC, Thompson PD, et al. Pathophysiology of bradykinesia in Parkinson's disease. *Brain* 2001;124:2131–46.
- [6] Williams, D. R. (2006). Predictors of falls and fractures in bradykinetic rigid syndromes: a retrospective study. *Journal of Neurology, Neurosurgery & Psychiatry*, 77(4), 468–473. doi:10.1136/jnnp.2005.074070.
- [7] Bloem B. Postural instability in Parkinson's disease. *Clinical neurology and neurosurgery*. 1992;94:41-5
- [8] Jauhiainen, M., Puustinen, J., Mehrang, S., Ruokolainen, J., Holm, A., Vehkaoja, A. and Nieminen, H. (2019). Identification of Motor Symptoms Related to Parkinson Disease Using Motion-Tracking Sensors at Home (KÄVELI): Protocol for an Observational Case-Control Study. *JMIR Research Protocols*, 8(3), p.e12808.
- [9] Goetz CG, Tilley BC, Shaftman SR, Stebbins GT, Fahn S, Martinez-Martin P, et al. Movement Disorder Society-sponsored revision of the Unified Parkinson's Disease Rating Scale (MDS-UPDRS): scale presentation and clinical testing results. *Movement disorders: official journal of the Movement Disorder Society*. 2008;23(15):2129-70.
- [10] Koop, M., Shivitz, N. and Brontë-Stewart, H. (2008). Quantitative measures of fine motor, limb, and postural bradykinesia in very early stage, untreated Parkinson's disease. *Movement Disorders*, 23(9), pp.1262-1268.

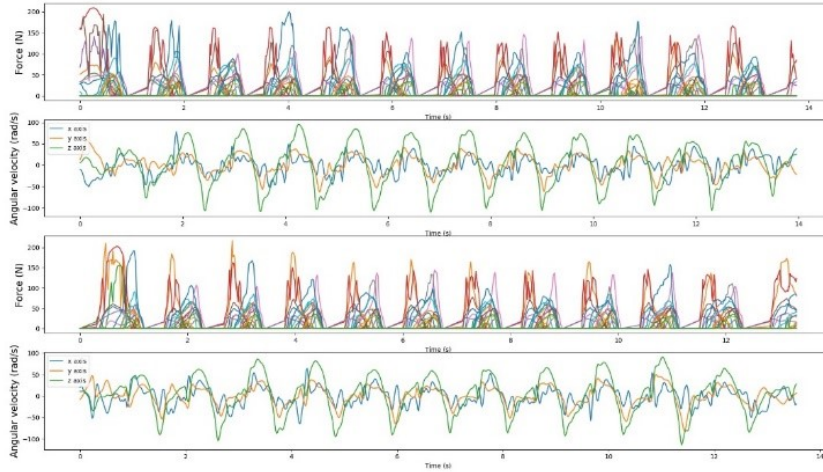
- [11] Rissanen, S., Kankaanpää, M., Meigal, A., Tarvainen, M., Nuutinen, J., Tarkka, I., Airaksinen, O. and Karjalainen, P. (2008). Surface EMG and acceleration signals in Parkinson's disease: feature extraction and cluster analysis. *Medical & Biological Engineering & Computing*, 46(9), pp.849-858.
- [12] Morris, M., Huxham, F., McGinley, J., Dodd, K. and Iansek, R. (2001). The biomechanics and motor control of gait in Parkinson disease. *Clinical Biomechanics*, 16(6), pp.459-470.
- [13] Martin P. *The basal ganglia and posture*. London: Pitman medical; 1967.
- [14] Murray MP, Sepic SB, Gardner GM, Downes WJ. Walking patterns of men with Parkinsonism. *Amer J Phys Med* 1987;278-94.
- [15] Sofuwa, O., Nieuwboer, A., Desloovere, K., Willems, A., Chavret, F. and Jonkers, I. (2005). Quantitative Gait Analysis in Parkinson's Disease: Comparison With a Healthy Control Group. *Archives of Physical Medicine and Rehabilitation*, 86(5), pp.1007-1013.
- [16] Morris ME, McGinley J, Huxham F, Collier J, Iansek R. Constraints on the kinetic, kinematic and spatiotemporal parameters of gait in Parkinson's disease. *Hum Mov Sci* 1999;18:461-83.
- [17] Nieuwboer A, De Weerd W, Dom R, et al. Plantar force distribution in parkinsonian gait: a comparison between patients and age-matched control subjects. *Scand J Rehabil Med* 1999;31:185- 92.
- [18] Schlachetzki, J., Barth, J., Marxreiter, F., Gossler, J., Kohl, Z., Reinfelder, S., Gassner, H., Aminian, K., Eskofier, B., Winkler, J. and Klucken, J. (2017). Wearable sensors objectively measure gait parameters in Parkinson's disease. *PLOS ONE*, 12(10), p.e0183989.
- [19] Healthline. (2019). Cogwheeling in Parkinson's Disease: Causes and Treatment. [online] Available at: <https://www.healthline.com/health/cogwheeling> [Accessed 29 Apr. 2019].
- [20] Mazilu, S., Blanke, U., Calatroni, A., Gazit, E., Hausdorff, J. and Tröster, G. (2016). The role of wrist-mounted inertial sensors in detecting gait freeze episodes in Parkinson's disease. *Pervasive and Mobile Computing*, 33, pp.1-16.
- [21] San-Segundo, R., Torres-Sánchez, R., Hodgins, J. and De la Torre, F. (2019). Increasing Robustness in the Detection of Freezing of Gait in Parkinson's Disease. *Electronics*, 8(2), p.119.
- [22] Nutt, J., Bloem, B., Giladi, N., Hallett, M., Horak, F. and Nieuwboer, A. (2011). Freezing of gait: moving forward on a mysterious clinical phenomenon. *The Lancet Neurology*, 10(8), pp.734-744.

- [23] Giladi, N. and Nieuwboer, A. (2008). Understanding and treating freezing of gait in parkinsonism, proposed working definition, and setting the stage. *Movement Disorders*, 23(S2), pp. S423-S425.
- [24] Son, D., Lee, J., Qiao, S., Ghaffari, R., Kim, J., Lee, J. E., ... Kim, D.-H. (2014). Multifunctional wearable devices for diagnosis and therapy of movement disorders. *Nature Nanotechnology*, 9(5), 397–404. doi:10.1038/nnano.2014.38.
- [25] Bächlin, M., Plotnik, M., Roggen, D., Giladi, N., Hausdorff, J. M., & Tröster, G. (2009). A Wearable System to Assist Walking of Parkinson's Disease Patients. *Methods of Information in Medicine*. doi:10.3414/me09-02-0003.
- [26] Tsipouras MG, Tzallas AT, Rigas G, Tsouli S, Fotiadis DI, Konitsiotis S (2012) An automated methodology for levodopa-induced dyskinesia: assessment based on gyroscope and accelerometer signals. *Artif Intell Med* 55(2):127–135.
- [27] Maetzler W, Domingos J, Sruļijes K, Ferreira JJ, Bloem BR (2013) Quantitative wearable sensors for objective assessment of Parkinson's disease. *Mov Disord* 28(12):1628–1637.
- [28] Louter M, Maetzler W, Prinzen J, van Lummel RC, Hobert M, Arends JB, Bloem BR, Streffer J, Berg D, Overeem S, Liepelt-Scarfone I (2015) Accelerometer-based quantitative analysis of axial nocturnal movements differentiates patients with Parkinson's disease, but not high-risk individuals, from controls. *J Neurol Neurosurg Psychiatry* 86(1):32–37.
- [29] Del Din S, Godfrey A, Rochester L (2015) Validation of an accelerometer to quantify a comprehensive battery of gait characteristics in healthy older adults and Parkinson's disease: toward clinical and at home use. *IEEE J Biomed Health Inform*.

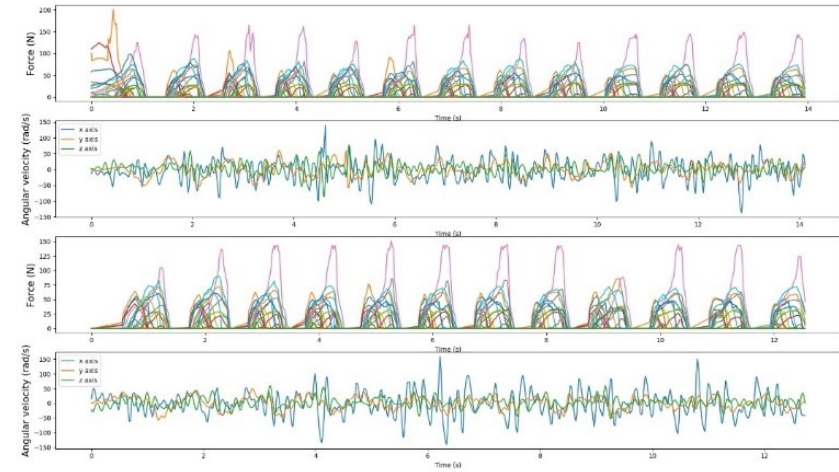
APPENDIX A: FIGURES

Cut data: Forciot data (N) together with the Suunto data (rad/s) plotted together per tests, first two from test 1 and last two from test 2, against time.

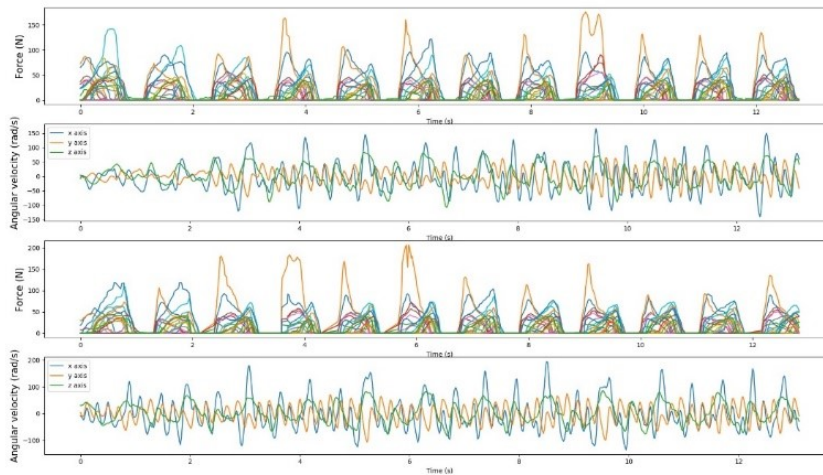
Subject Kav110. UPDRS 1,5



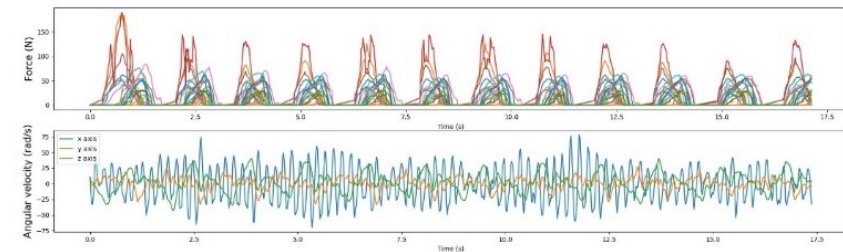
Subject Kav096. UPDRS 2,5



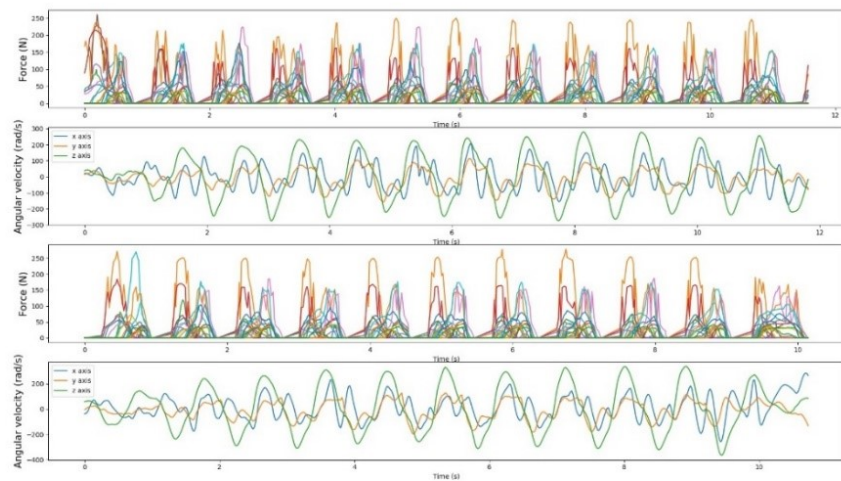
Subject Kav112. UPDRS 3



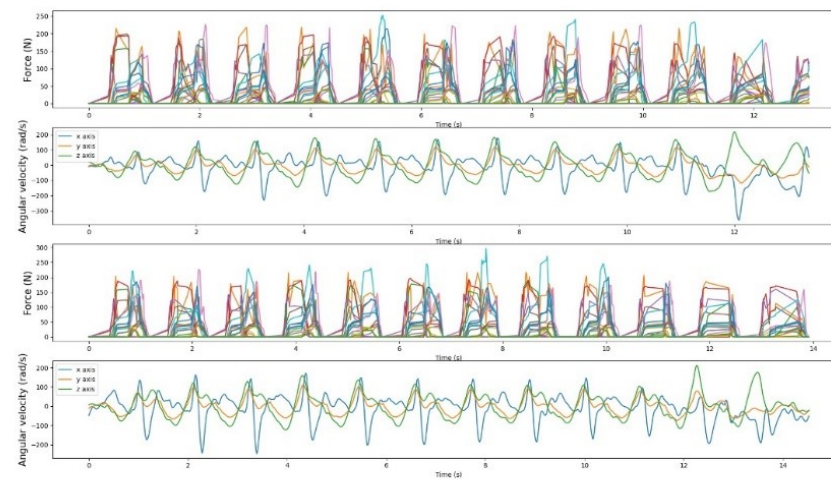
Subject Kav042. UPDRS 4



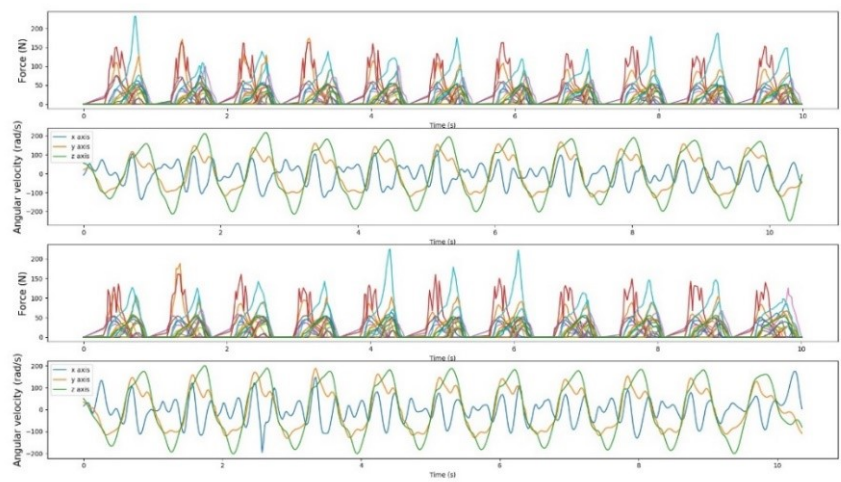
Subject Kav113. UPDRS 0



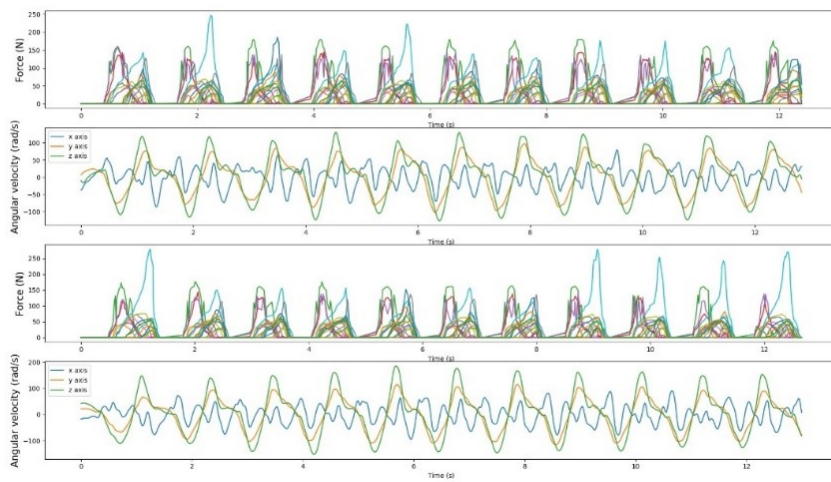
Subject Kav114. UPDRS 0



Subject Kav138. UPDRS 0

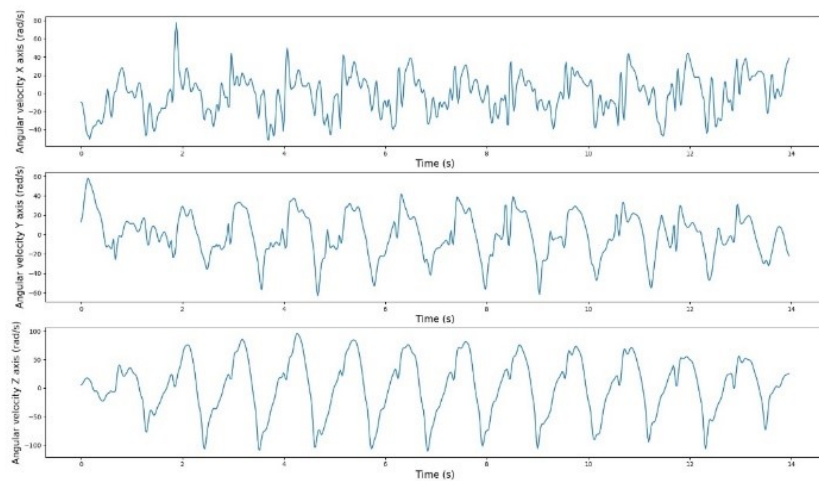


Subject Kav175. UPDRS 0

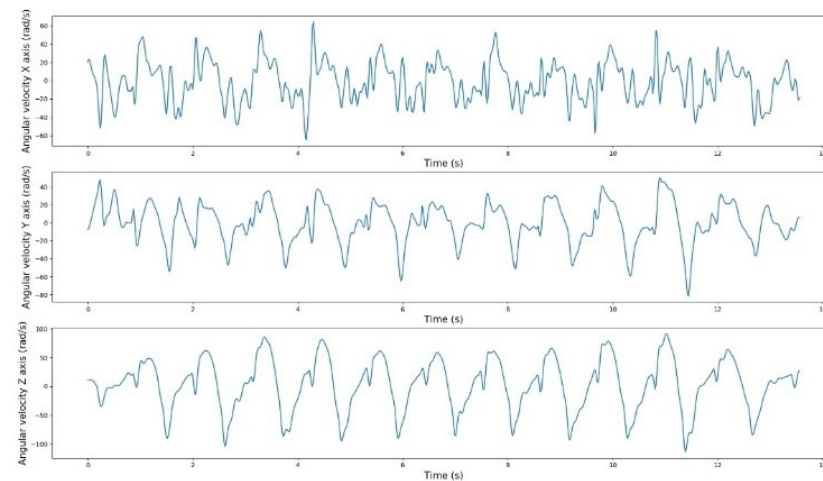


Cut Suunto data per axis: Angular velocity measured around the three axes, X (top), Y (center) and Z (bottom).

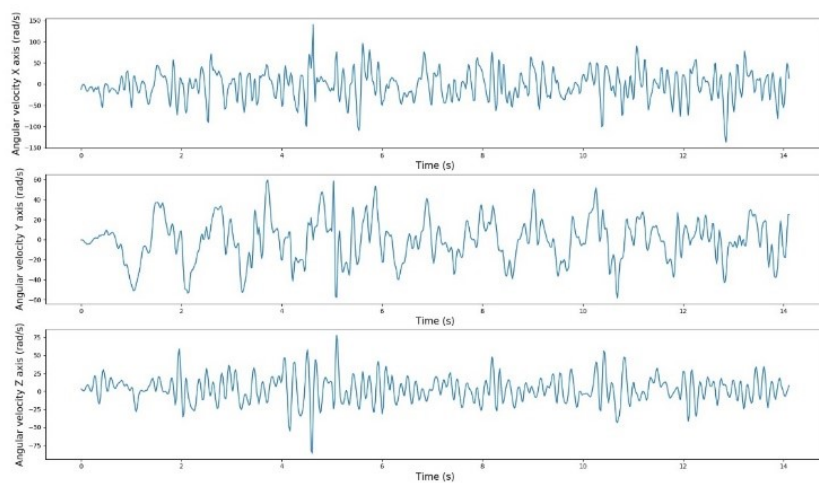
Subject Kav110. UPDRS 1,5. Test: 1



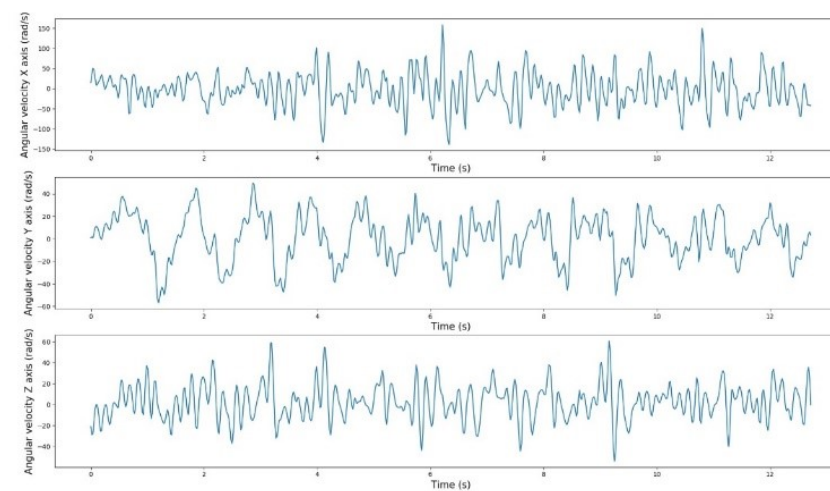
Subject Kav110. UPDRS 1,5. Test: 2



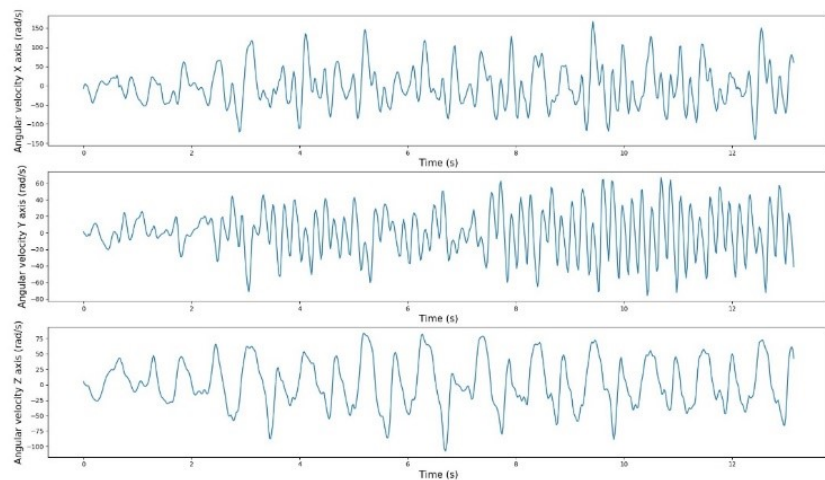
Subject Kav096. UPDRS 2,5. Test: 1



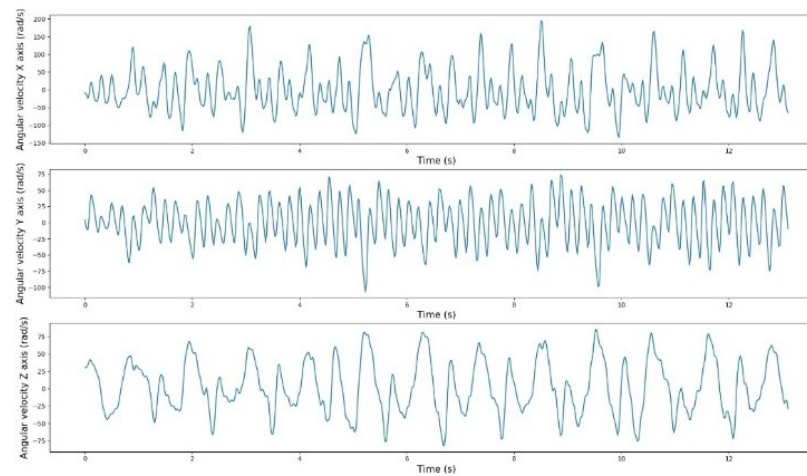
Subject Kav096. UPDRS 2,5. Test: 2



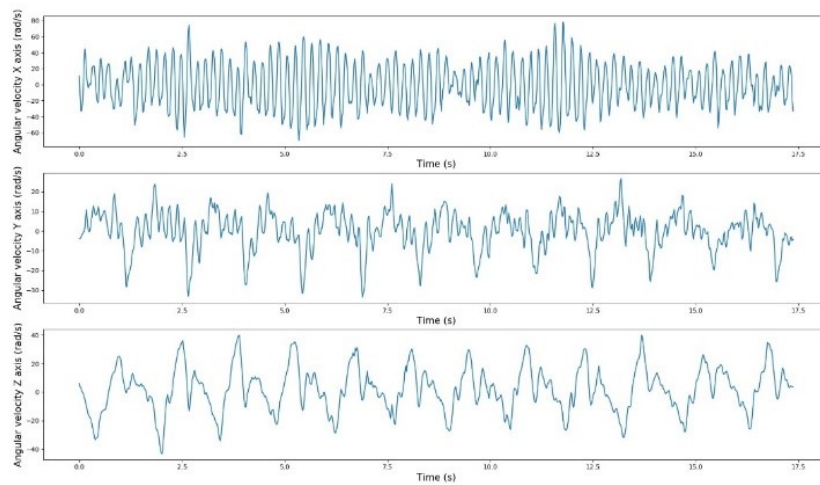
Subject Kav112. UPDRS 3. Test: 1



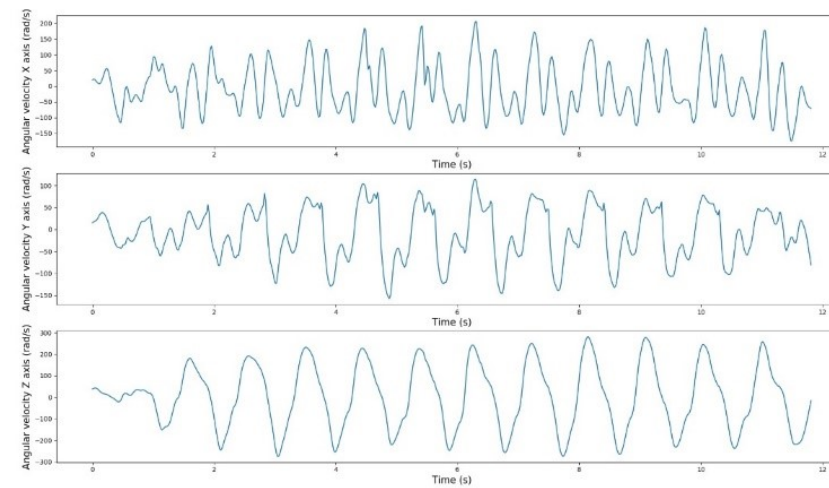
Subject Kav112. UPDRS 3. Test: 2



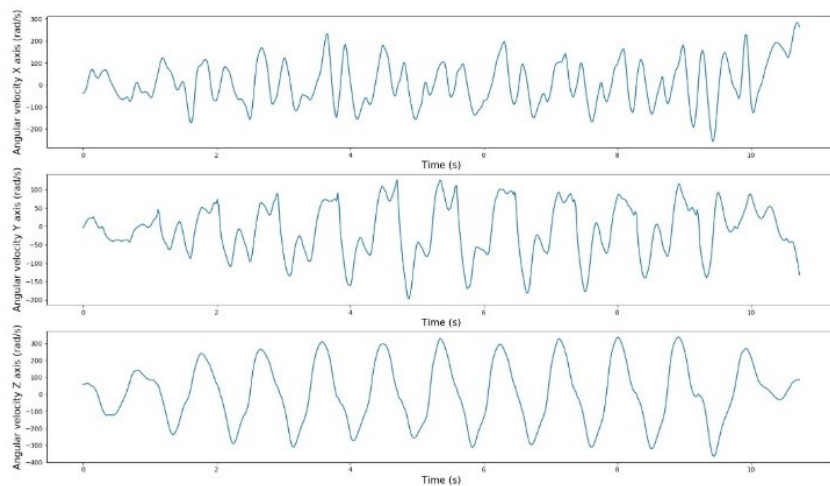
Subject Kav042. UPDRS 4. Test: 1



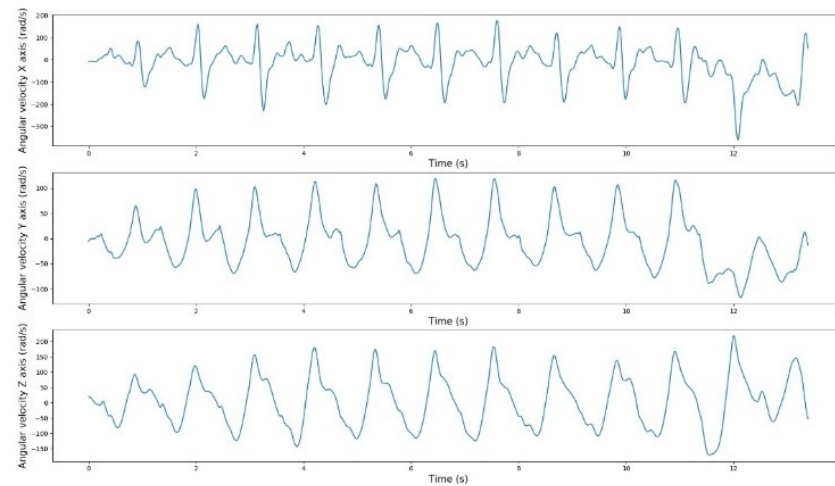
Subject Kav113. UPDRS 0. Test: 1



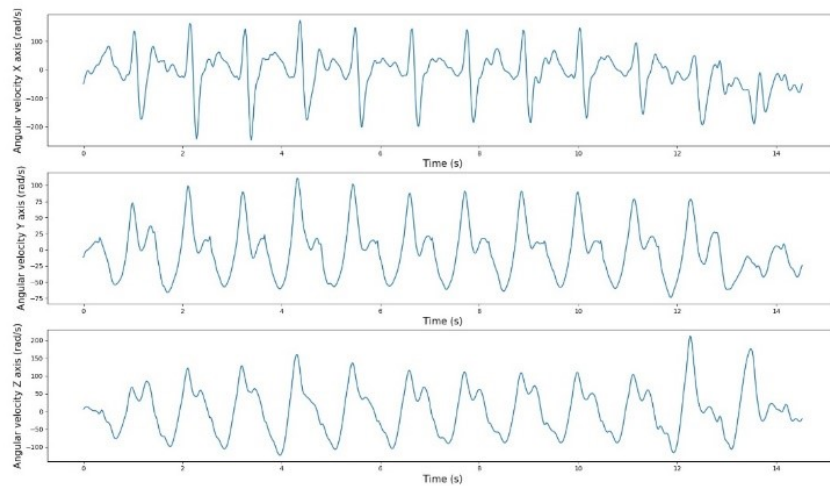
Subject Kav113. UPDRS 0. Test: 2



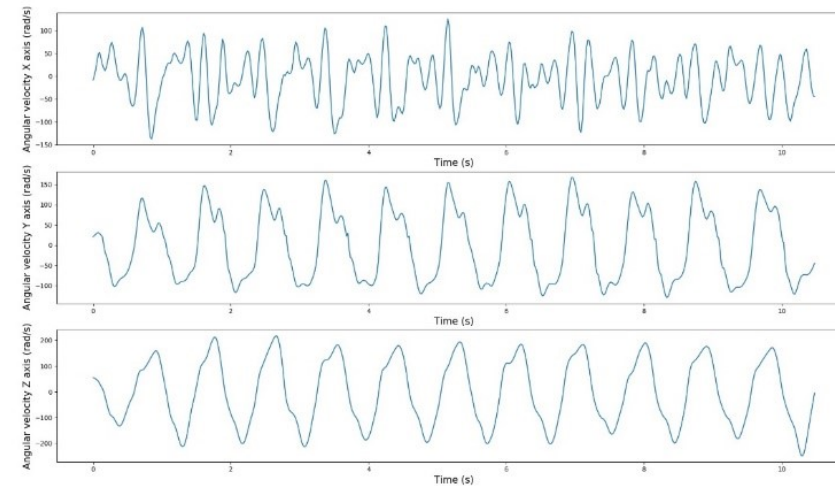
Subject Kav114. UPDRS 0. Test: 1



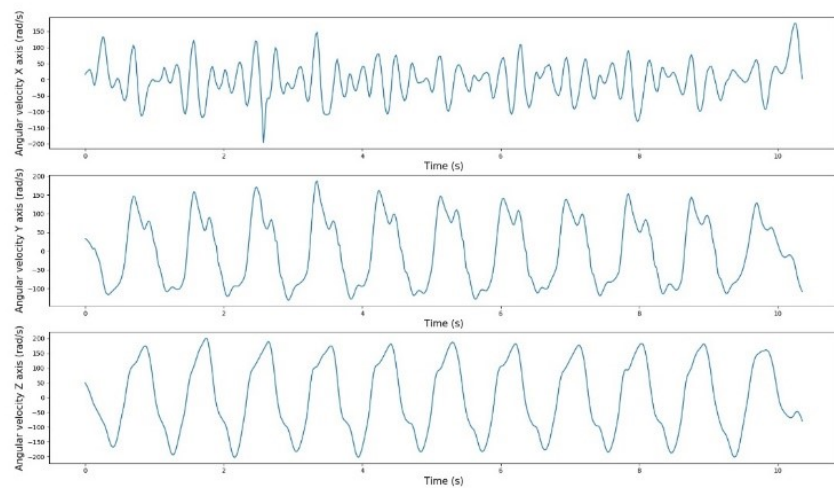
Subject Kav114. UPDRS 0. Test: 2



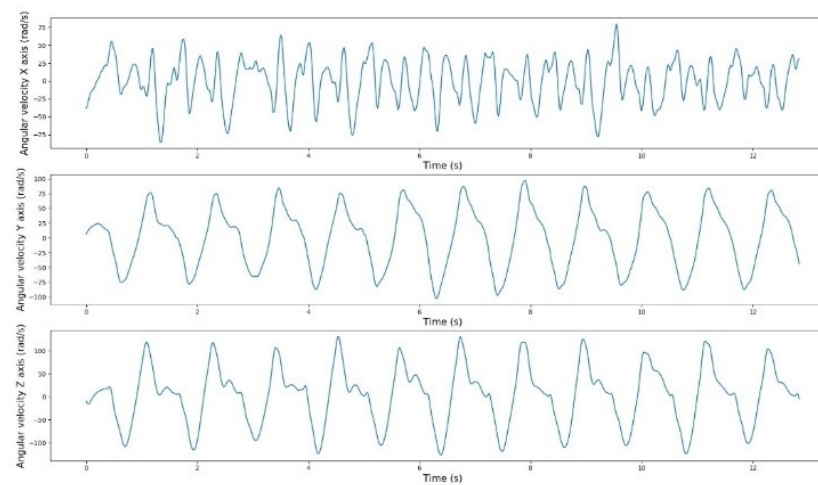
Subject Kav138. UPDRS 0. Test: 1



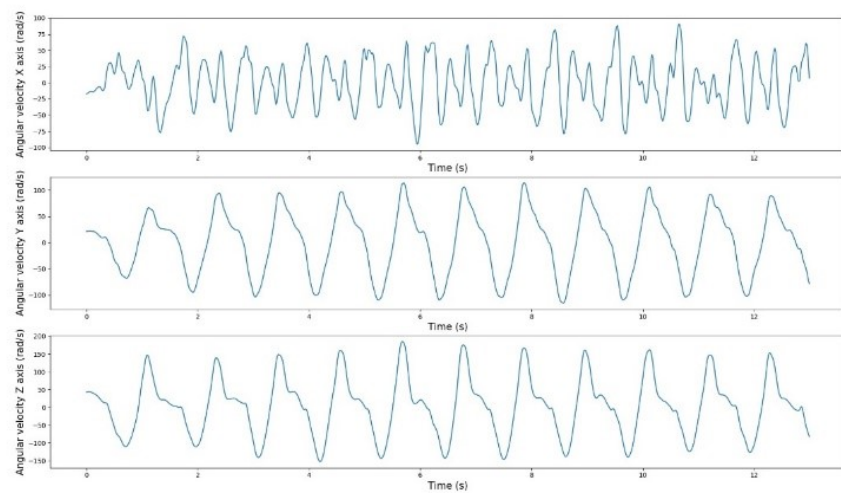
Subject Kav138. UPDRS 0. Test: 2



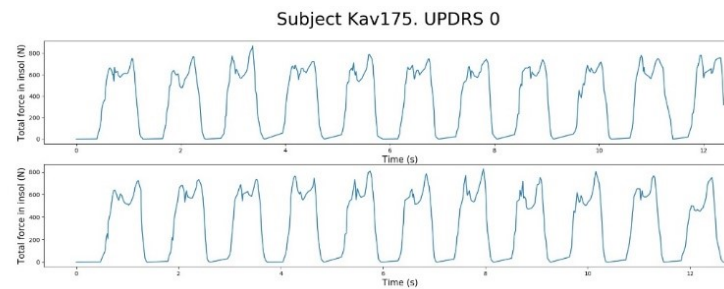
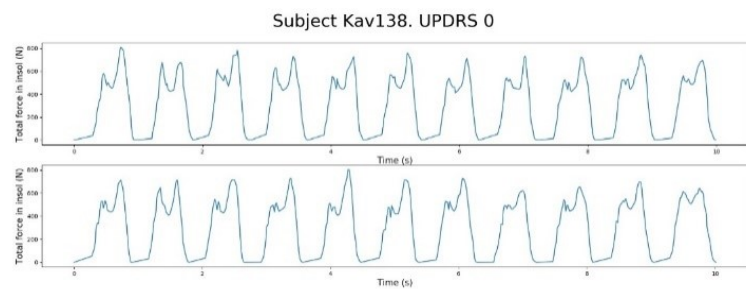
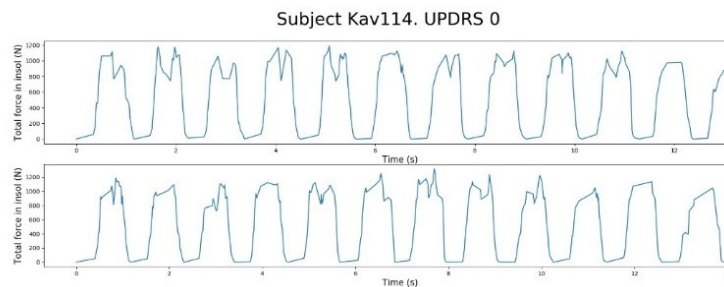
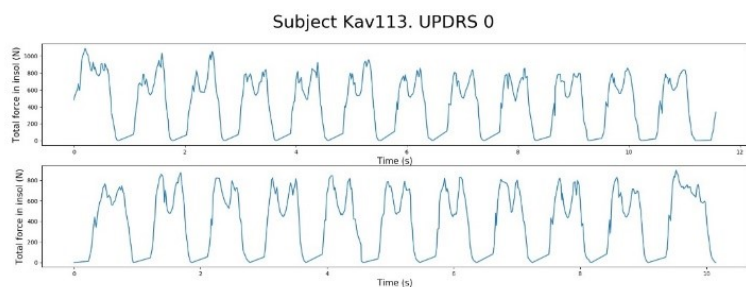
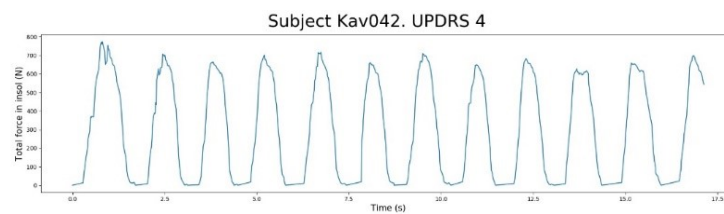
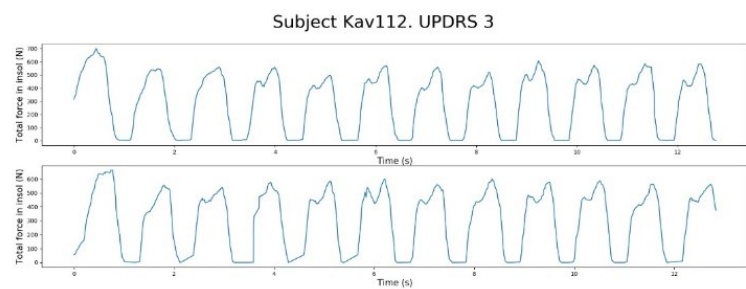
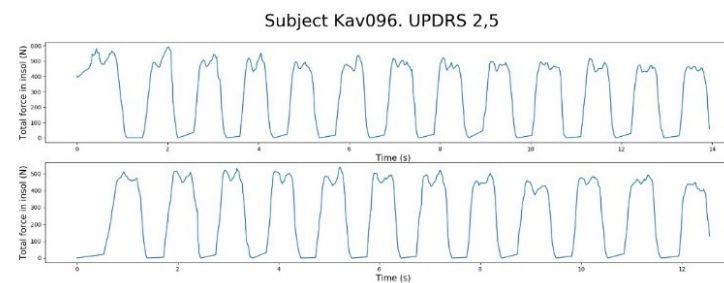
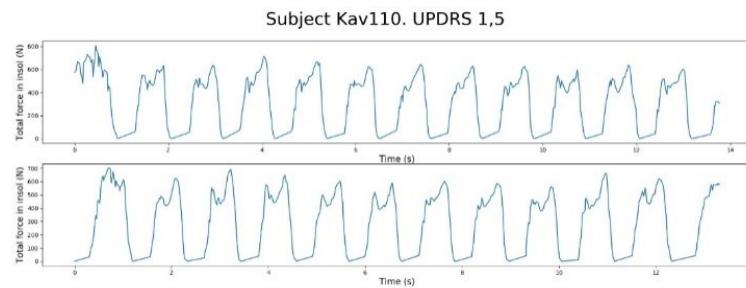
Subject Kav175. UPDRS 0. Test: 1



Subject Kav175. UPDRS 0. Test: 2

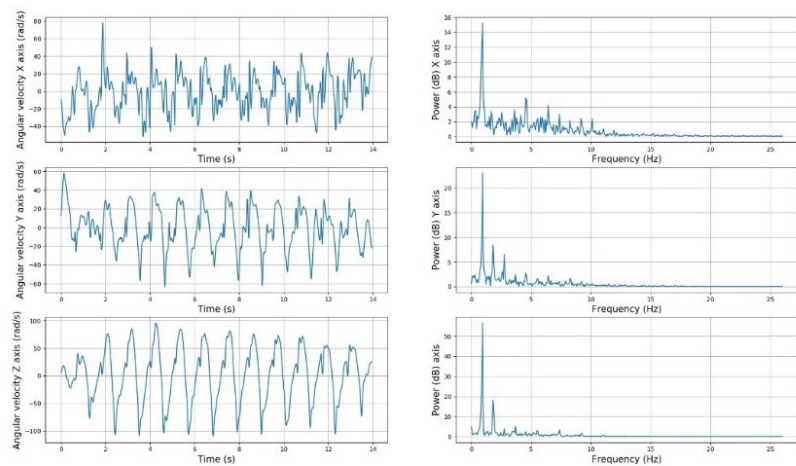


Forciot total input data: Total input data measured from Forciot insole (N). Test 1 (top) and test 2 (bottom).

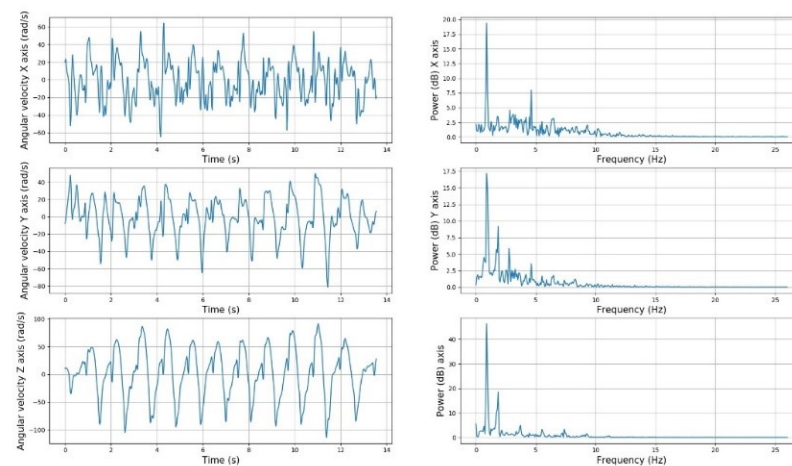


Suunto data analysis: Suunto data (rad/s) around the three axes. Time domain (left), frequency domain (right).

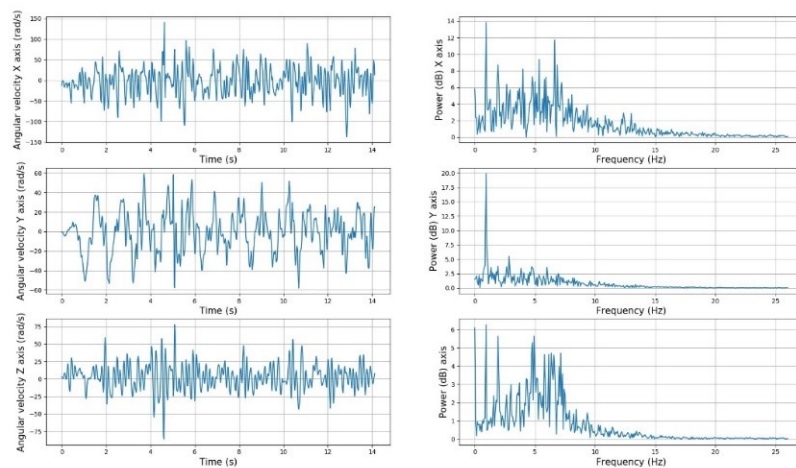
Subject Kav110. UPDRS 1,5. Test: 1



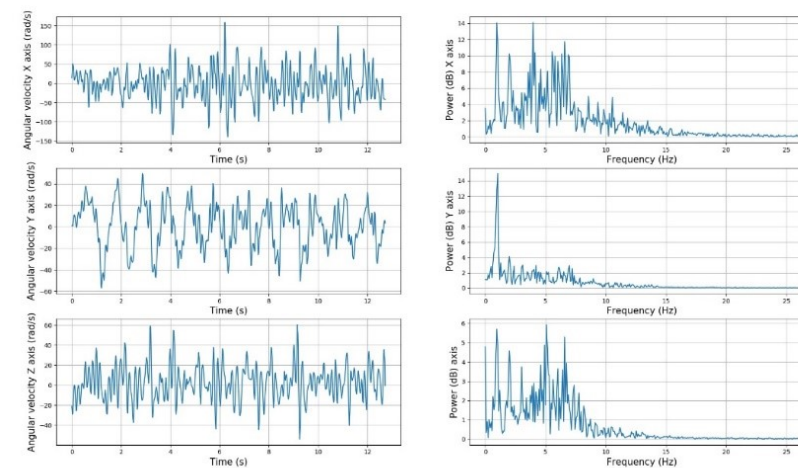
Subject Kav110. UPDRS 1,5. Test: 2



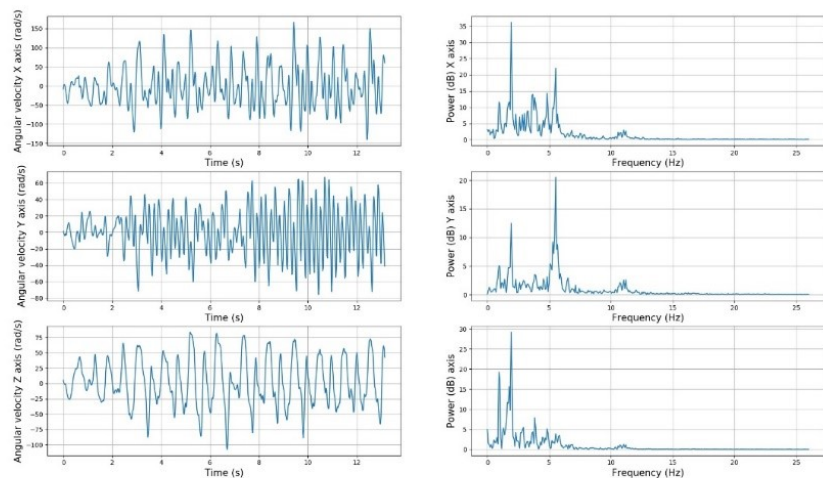
Subject Kav096. UPDRS 2,5. Test: 1



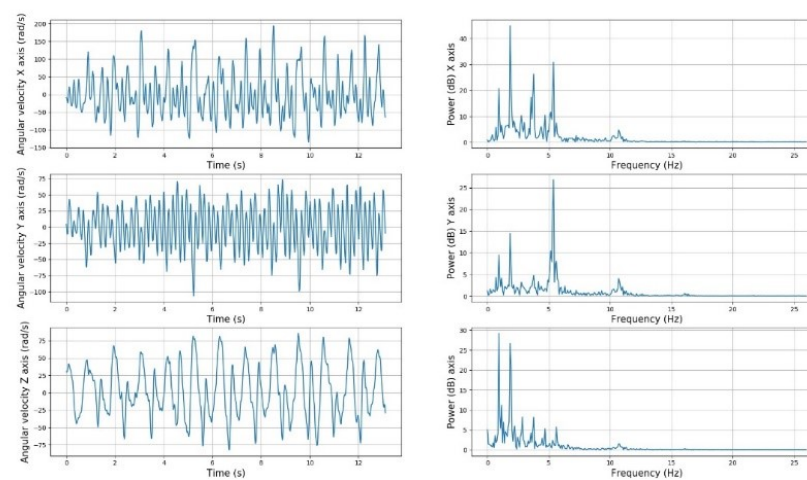
Subject Kav096. UPDRS 2,5. Test: 2



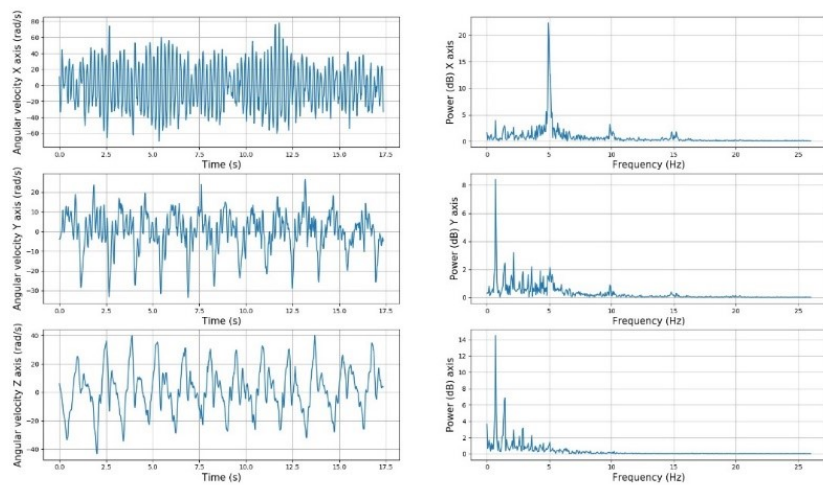
Subject Kav112. UPDRS 3. Test: 1



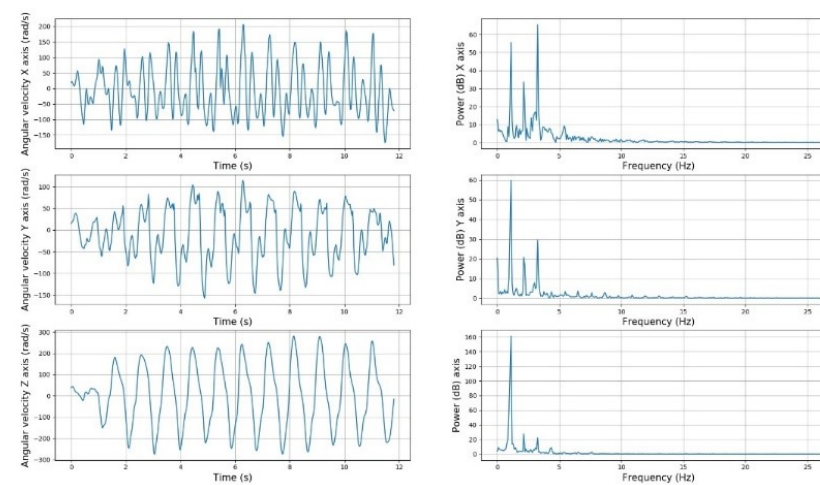
Subject Kav112. UPDRS 3. Test: 2



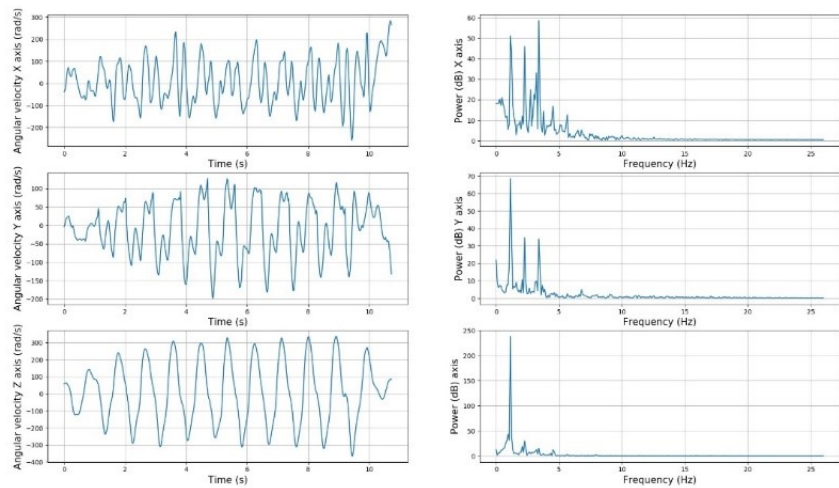
Subject Kav042. UPDRS 4. Test: 1



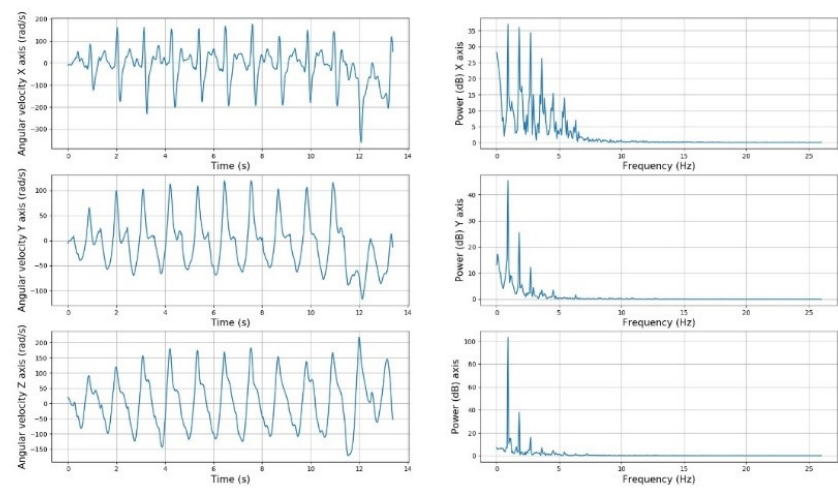
Subject Kav113. UPDRS 0. Test: 1



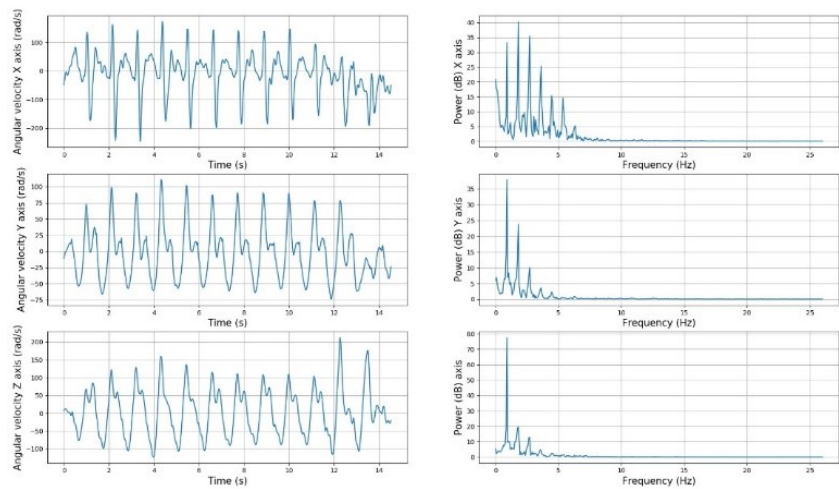
Subject Kav113. UPDRS 0. Test: 2



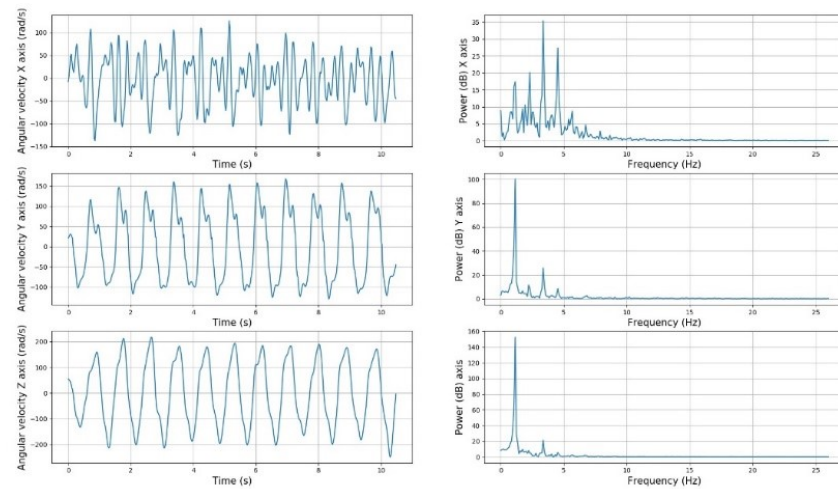
Subject Kav114. UPDRS 0. Test: 1



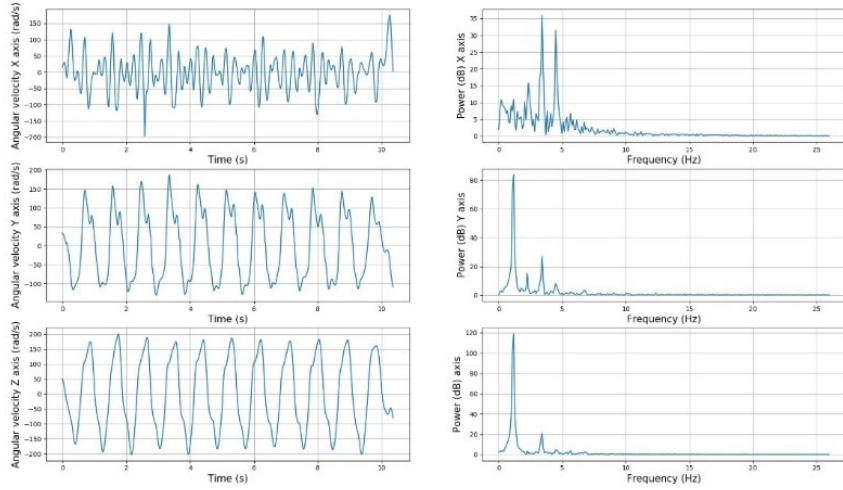
Subject Kav114. UPDRS 0. Test: 2



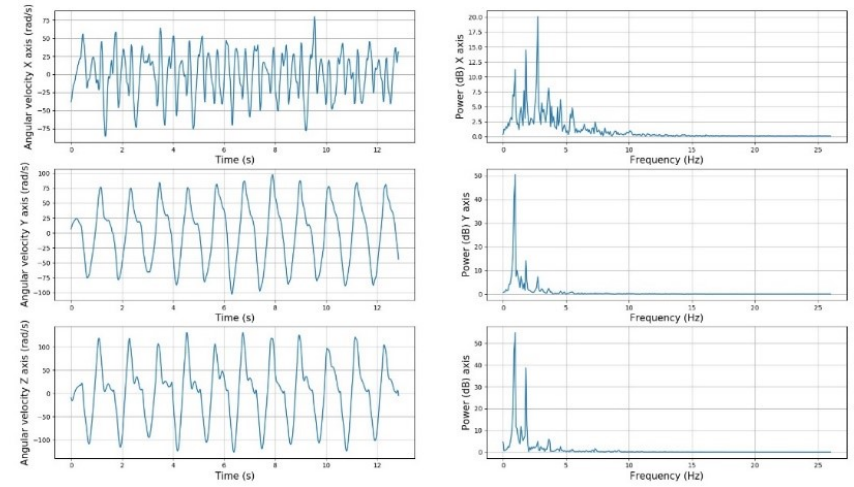
Subject Kav138. UPDRS 0. Test: 1



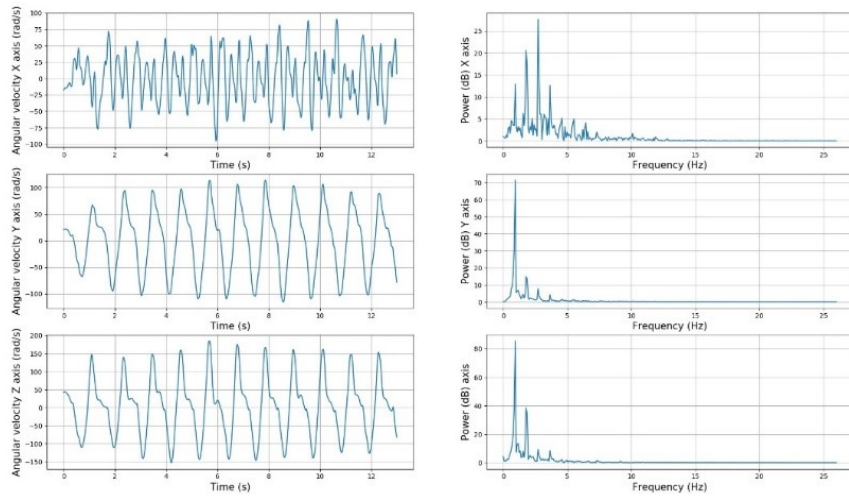
Subject Kav138. UPDRS 0. Test: 2



Subject Kav175. UPDRS 0. Test: 1

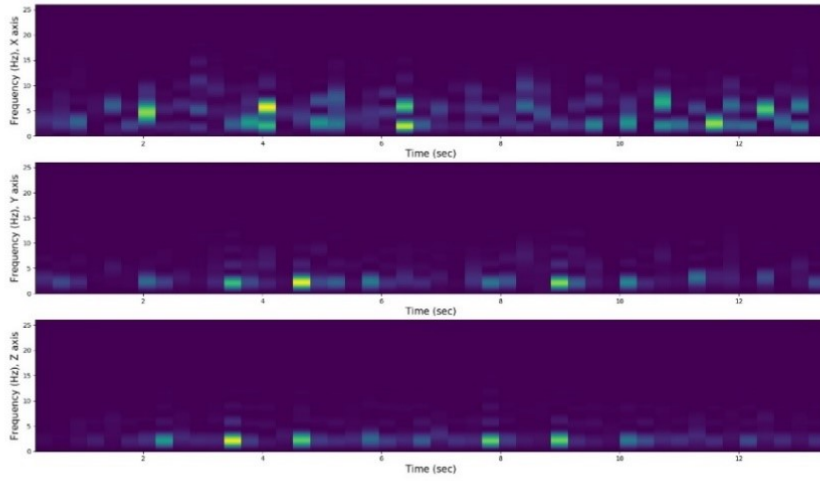


Subject Kav175. UPDRS 0. Test: 2

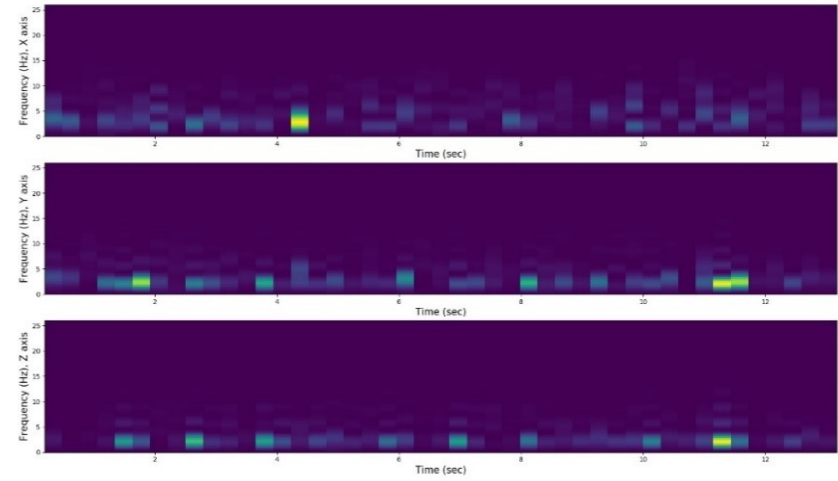


Suunto Spectrograms: Spectrograms of the angular velocity around the three axes, X (top), Y (center) and Z (bottom).

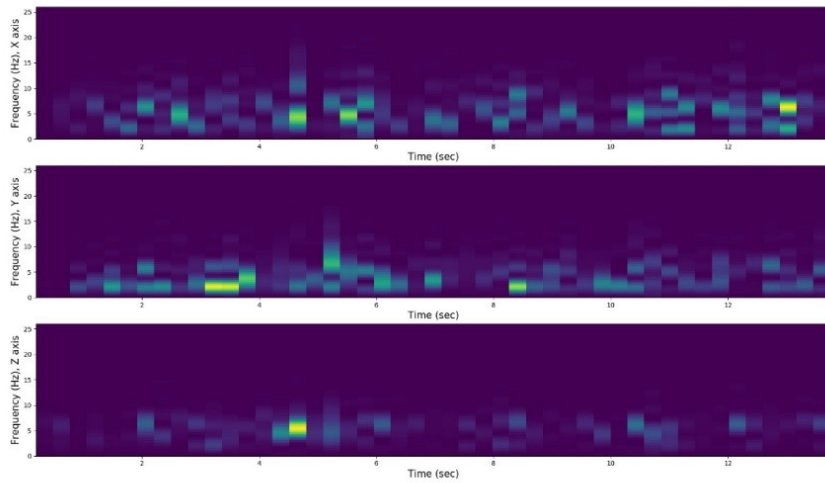
Subject Kav110. UPDRS 1,5. Test: 1. Suunto Gyroscope Spectrogram



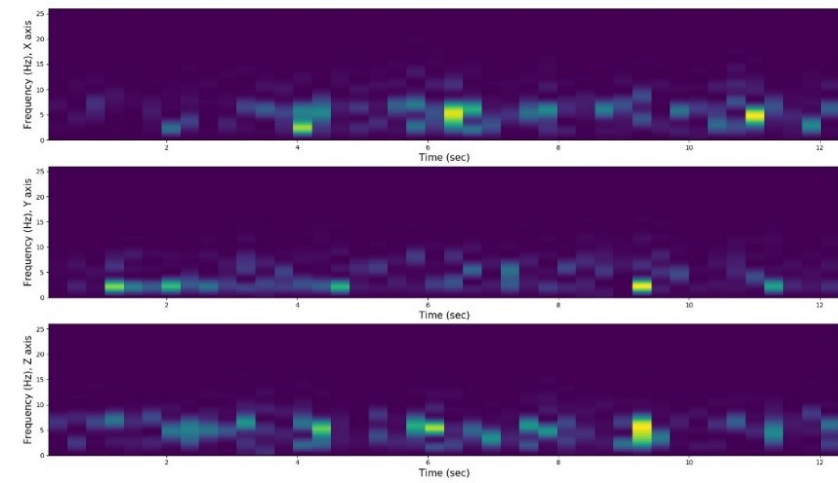
Subject Kav110. UPDRS 1,5. Test: 2. Suunto Gyroscope Spectrogram



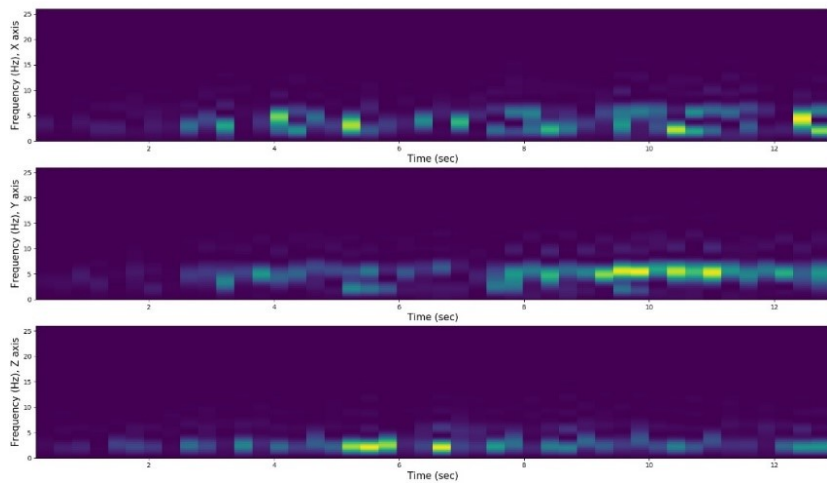
Subject Kav096. UPDRS 2,5. Test: 1. Suunto Gyroscope Spectrogram



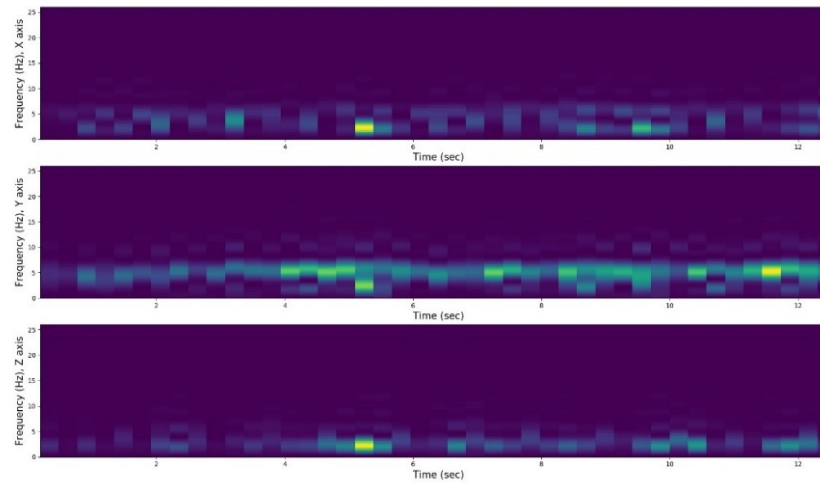
Subject Kav096. UPDRS 2,5. Test: 2. Suunto Gyroscope Spectrogram



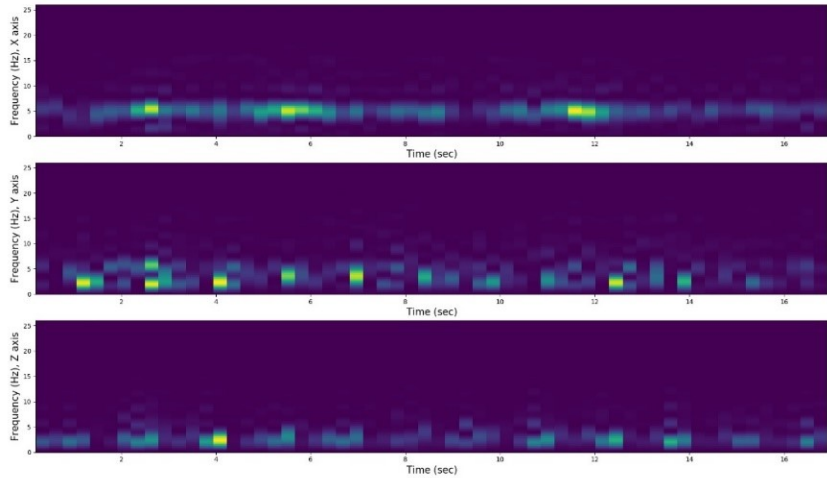
Subject Kav112. UPDRS 3. Test: 1. Suunto Gyroscope Spectrogram



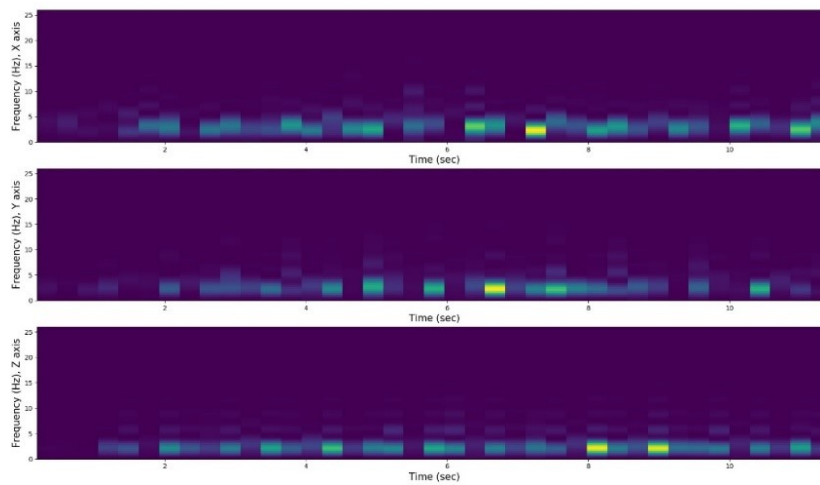
Subject Kav112. UPDRS 3. Test: 2. Suunto Gyroscope Spectrogram



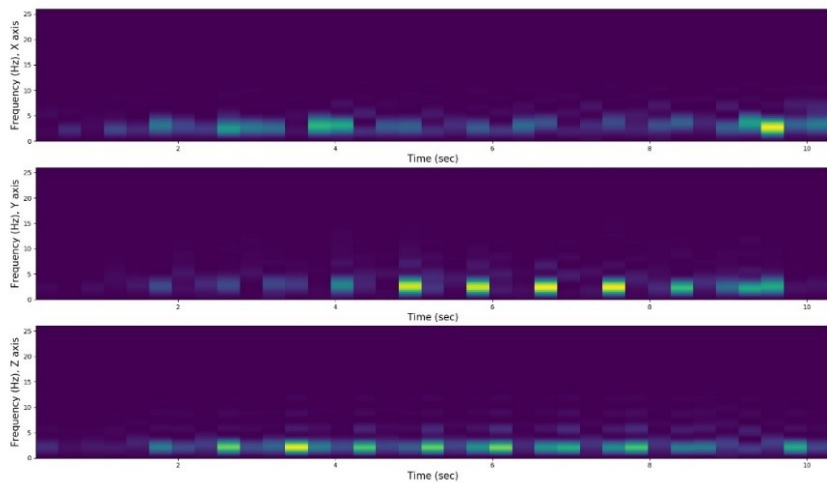
Subject Kav042. UPDRS 4. Test: 1. Suunto Gyroscope Spectrogram



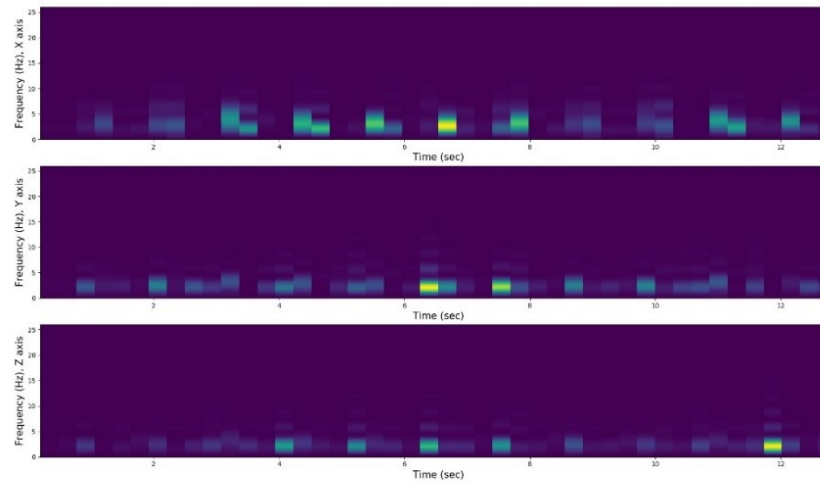
Subject Kav113. UPDRS 0. Test: 1. Suunto Gyroscope Spectrogram



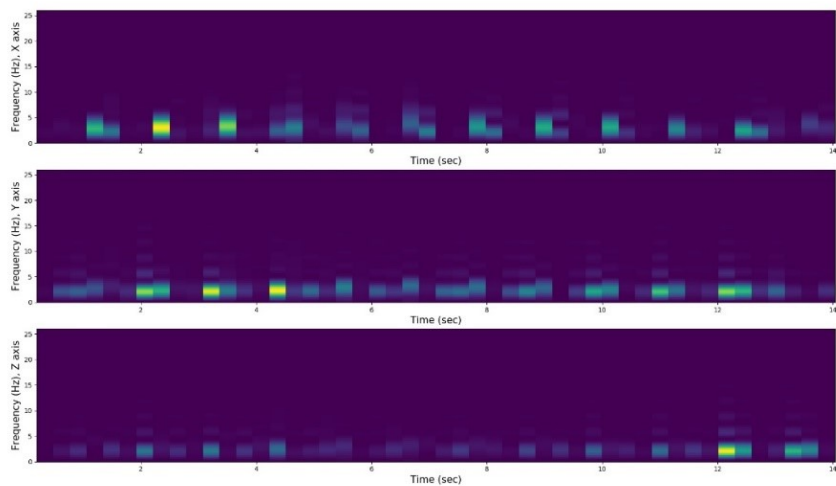
Subject Kav113. UPDRS 0. Test: 2. Suunto Gyroscope Spectrogram



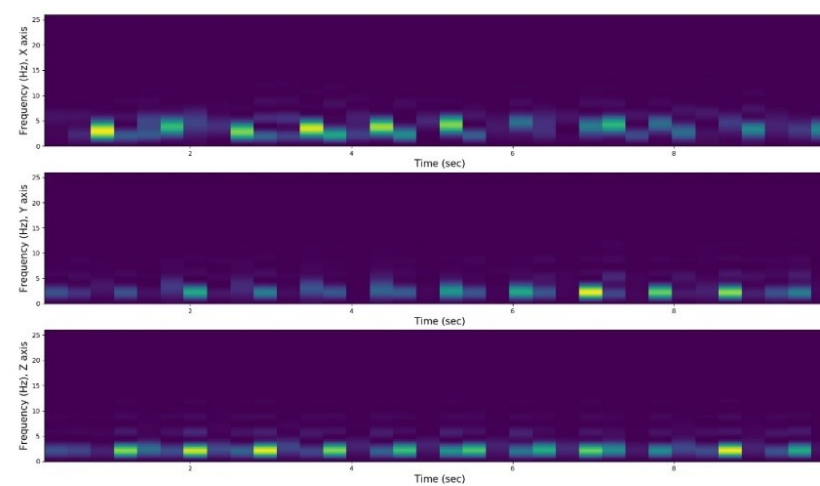
Subject Kav114. UPDRS 0. Test: 1. Suunto Gyroscope Spectrogram



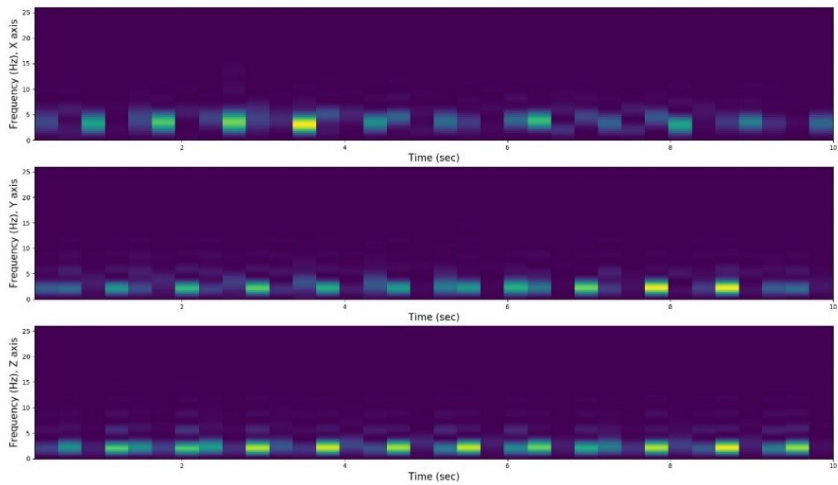
Subject Kav114. UPDRS 0. Test: 2. Suunto Gyroscope Spectrogram



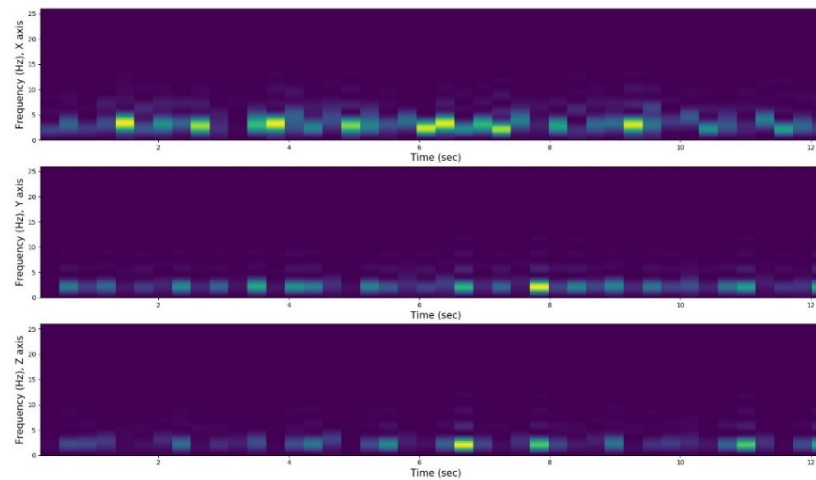
Subject Kav138. UPDRS 0. Test: 1. Suunto Gyroscope Spectrogram



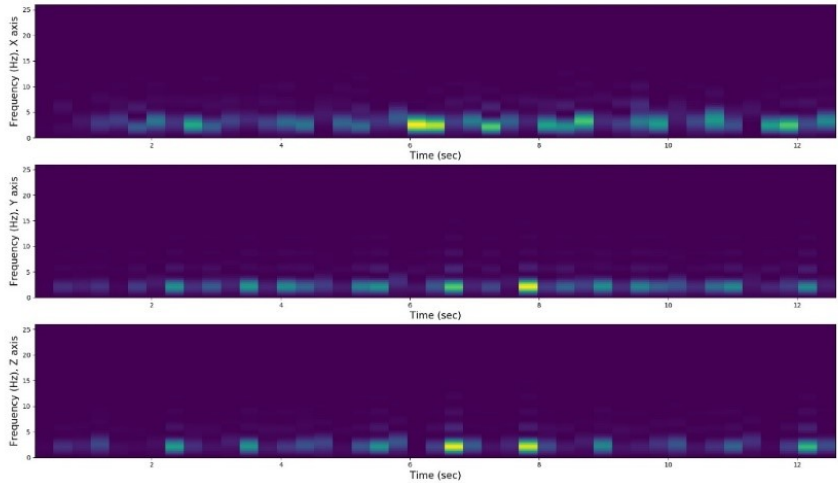
Subject Kav138. UPDRS 0. Test: 2. Suunto Gyroscope Spectrogram



Subject Kav175. UPDRS 0. Test: 1. Suunto Gyroscope Spectrogram

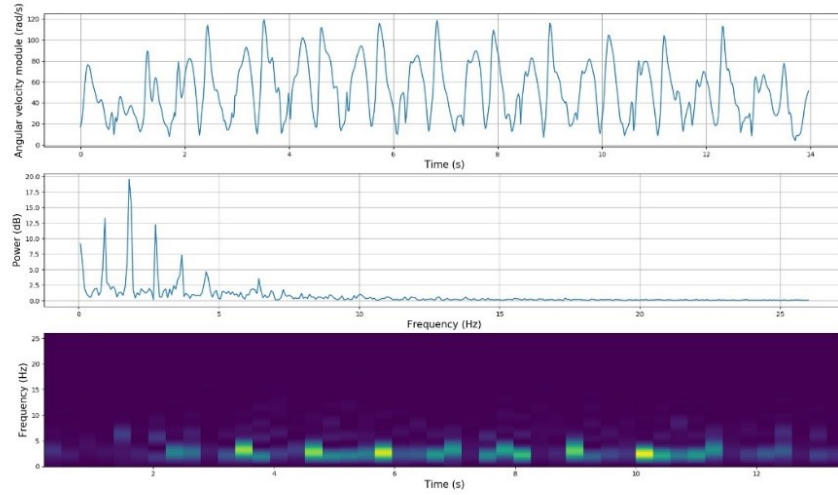


Subject Kav175. UPDRS 0. Test: 2. Suunto Gyroscope Spectrogram

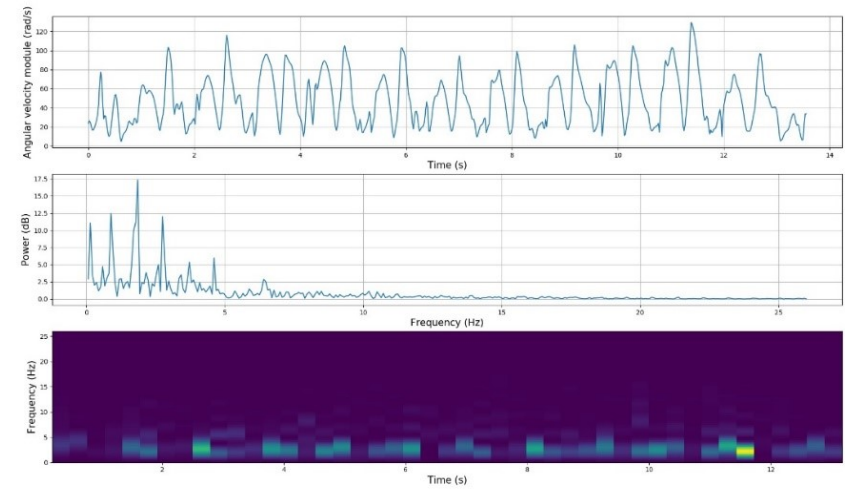


Suunto module: Representation of the angular velocity module in time domain (top), frequency domain (center) and its spectrogram (bottom).

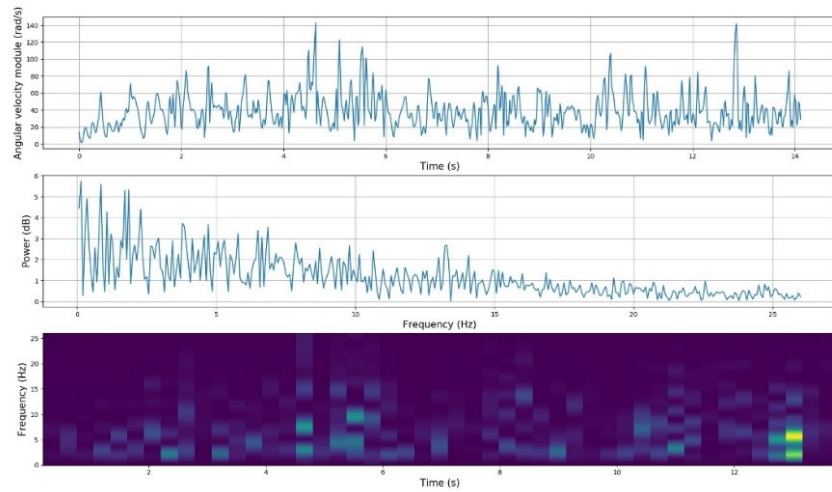
Subject Kav110. UPDRS 1,5. Test: 1. Angular Velocity Vector Module



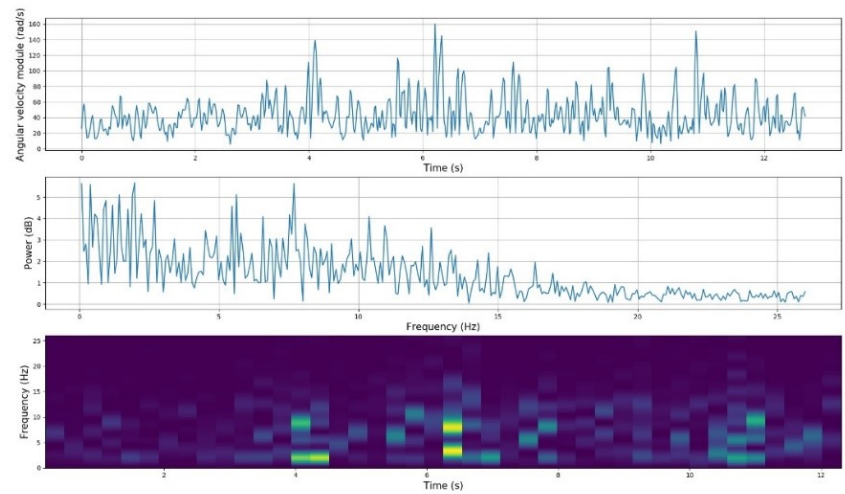
Subject Kav110. UPDRS 1,5. Test: 2. Angular Velocity Vector Module



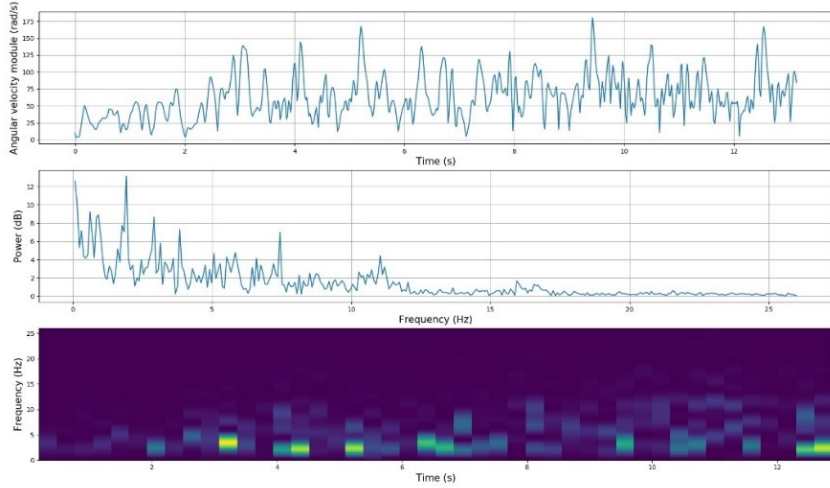
Subject Kav096. UPDRS 2,5. Test: 1. Angular Velocity Vector Module



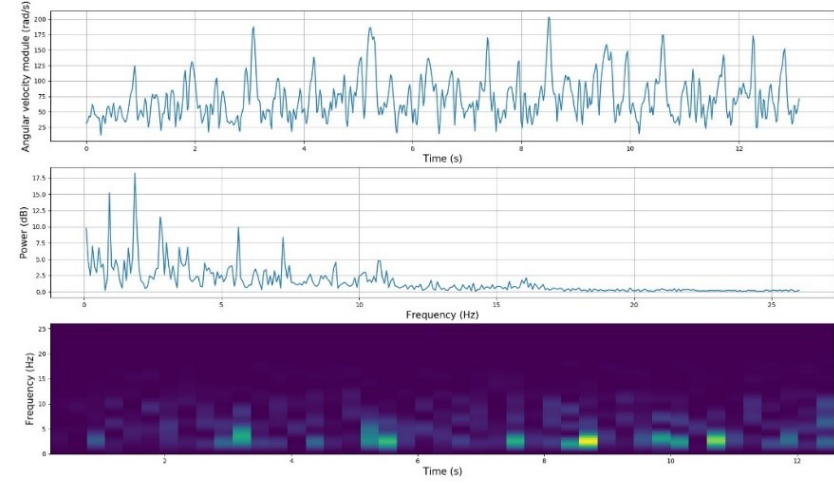
Subject Kav096. UPDRS 2,5. Test: 2. Angular Velocity Vector Module



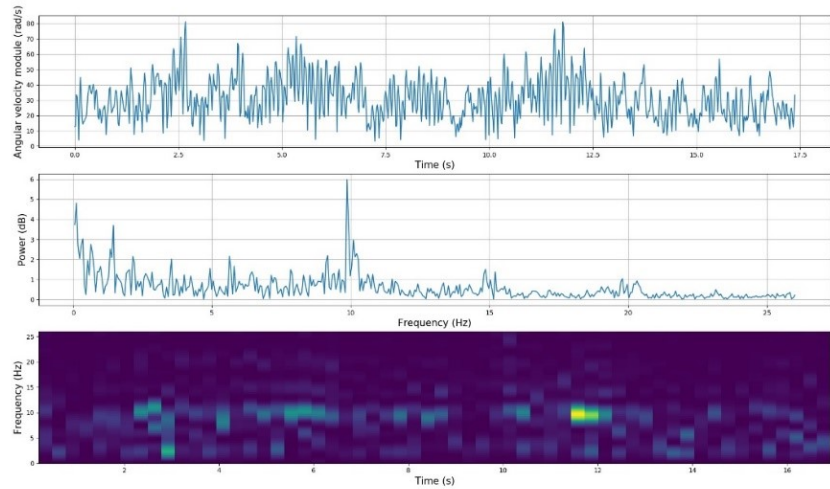
Subject Kav112. UPDRS 3. Test: 1. Angular Velocity Vector Module



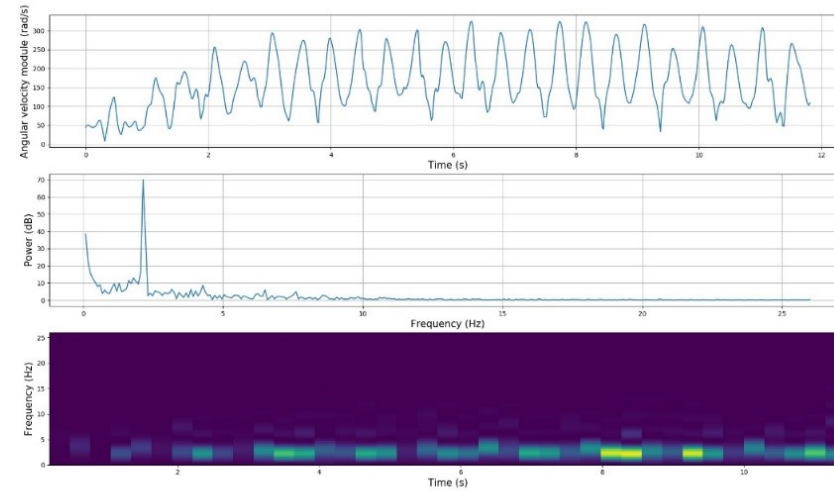
Subject Kav112. UPDRS 3. Test: 2. Angular Velocity Vector Module



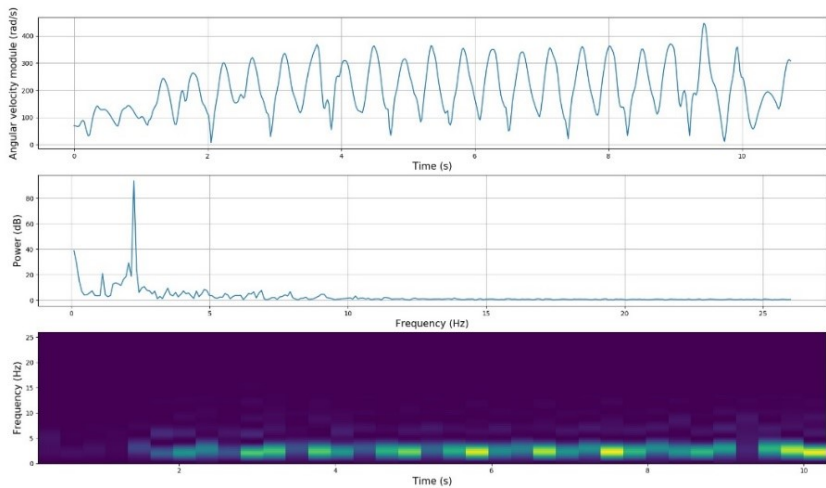
Subject Kav042. UPDRS 4. Test: 1. Angular Velocity Vector Module



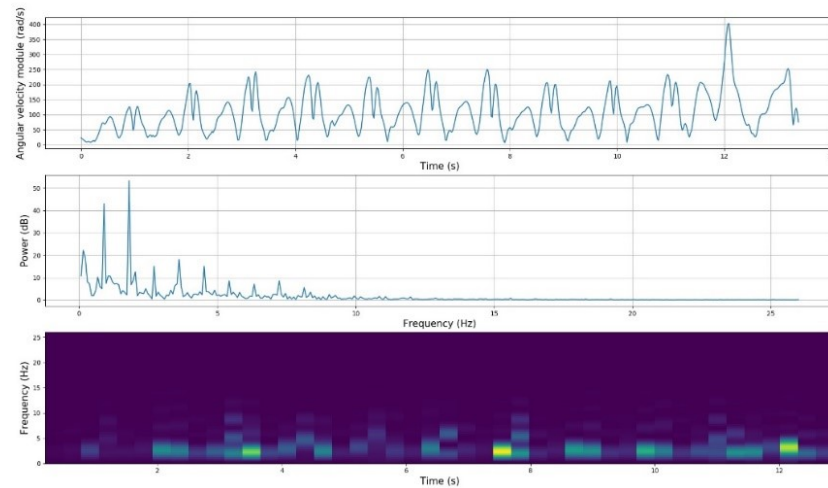
Subject Kav113. UPDRS 0. Test: 1. Angular Velocity Vector Module



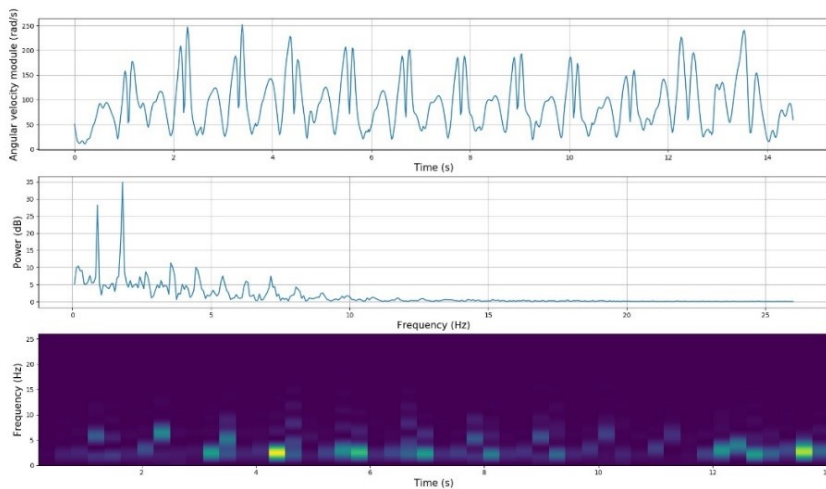
Subject Kav113. UPDRS 0. Test: 2. Angular Velocity Vector Module



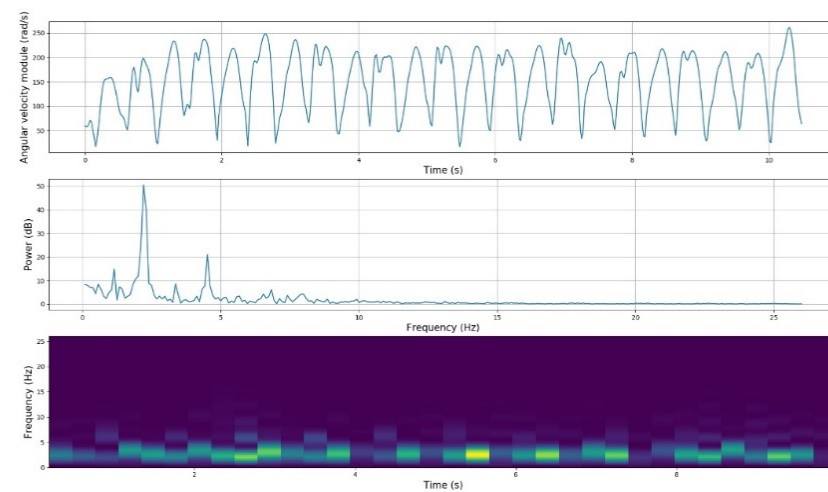
Subject Kav114. UPDRS 0. Test: 1. Angular Velocity Vector Module



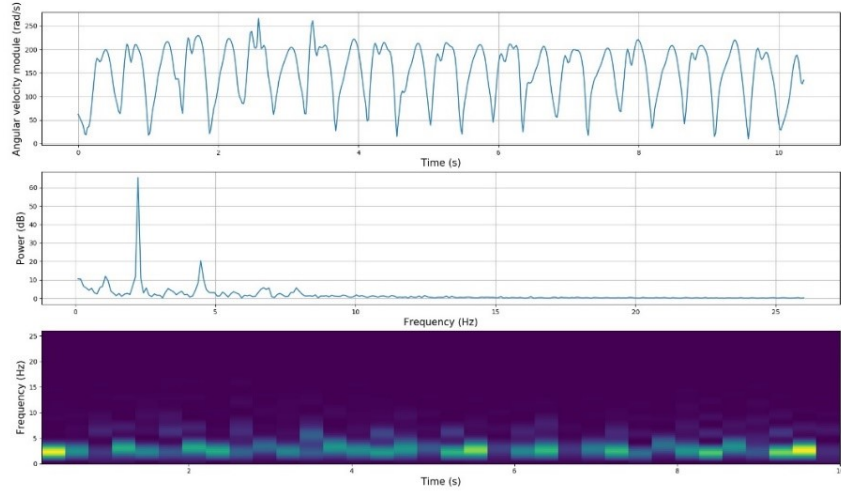
Subject Kav114. UPDRS 0. Test: 2. Angular Velocity Vector Module



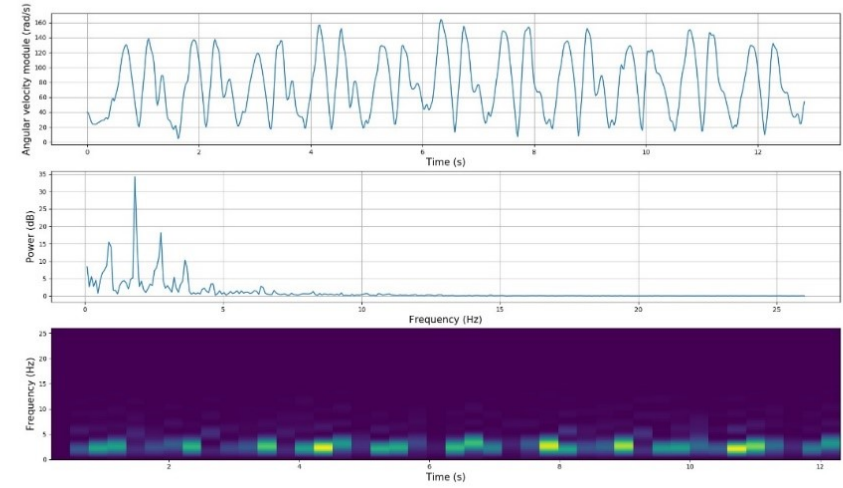
Subject Kav138. UPDRS 0. Test: 1. Angular Velocity Vector Module



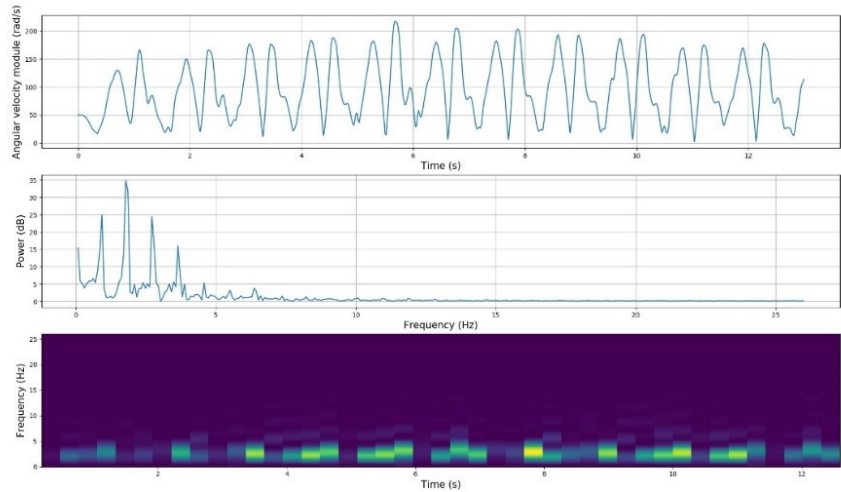
Subject Kav138. UPDRS 0. Test: 2. Angular Velocity Vector Module



Subject Kav175. UPDRS 0. Test: 1. Angular Velocity Vector Module



Subject Kav175. UPDRS 0. Test: 2. Angular Velocity Vector Module



APPENDIX B: ETHIC, SOCIAL, ECONOMIC AND ENVIRONMENTAL ASPECTS.

This appendix contains a brief explanation of some of the impacts that the subject of this thesis can have on ethical, social, economic and environmental aspects.

B.1 Introduction

Parkinson's disease is the second most common neurodegenerative disease. The symptoms encompass a range of features that go from motor disabilities to affect the patient's cognition. Even though there is no definite cure, there are treatments that help managing the symptoms in order to make life easier for the people suffering it by, for example, reducing the risk of accidents. The most common one is the treatment with levodopa. One of the greatest challenges is the correct application of the levodopa dosage since the severity of the symptoms is very variable by days (or even within the same one) and the inputs the clinicians have are from tests performed in the appointments with the patient, which is not representative of the state of the disease. Proper daily monitoring is a need in order to provide a more sufficient input on the state of the patient and the response to the treatment (i.e. the state before and after the levodopa dosage). Wearable technology can provide the information needed due to its low cost, and their higher comfort than bigger hospital devices.

This project uses a pressure sensitive insole and a gyroscopic sensor in the wrist of the subjects (4 in different stages of PD and 4 controls) to see if the motor symptoms of the disease can be detected and measured by the devices in a 20-step walking test. The interpretation of the data would be key for the clinicians to understand the stage of PD the patient is in.

B.2 Impact description related with the project

The main impacts related with this study can be classified as:

Social: Monitoring can be used to provide a more personalized treatment through medication and physiotherapy. This will result in an improvement the daily living activities performed by the patients.

Economic. The use of wearable technology in the assessment of PD motor symptoms can reduce the cost of the monitoring of the patients by having more thorough observation without increasing the number of visits to the hospital.

Ethical: The main ethical impact is the fact that in this project data is obtained from tests taken from human beings with Parkinson's Disease. Full consent is needed. There is another concern with the property of the data and the accessibility. Data was collected securely and remotely, without compromising the patient's privacy.

B.3 Expanded analysis of some of the impacts.

The daily monitoring can affect each patient's lives making more effective the treatment they are following, improving their daily life. They would be less dependent on the personal check ups and eventually, the data could be sent directly to the clinicians making the visit to the hospital less necessary.

As mention before, the use of wearable technology reduces the cost of the assessment of motor symptoms via more expensive hospital devices and the reduction of visits to the hospital reduces the overall price to treat the patient. Improving the effectiveness also reduces the cost in the dosage of levodopa since it avoids the use of extra dosage.

On the ethical part it should be noted that special care has to be taken because the study is based on data from PD patients. The project this study is based on was performed following the Ethical Principles for Medical Research Involving Human Subjects, revised version in 2013 of the World medical Association Declaration of Helsinki, Finland, in 1964. The data was coded and did not contain any kind of identifying information, to maintain the privacy of the subjects. The National Supervisory Authority of Welfare and Health in Helsinki (Valvira) approved the devices used in the study in April of 2018 and the study protocol was approved from the Ethics Committee of the Hospital District of Southwest Finland in Turku.

B.3 Conclusion

The socioeconomic impact of this project is not direct but rather is based on the effects it would have. The devices don't help in any direct manner to the daily living of the patients but they suppose a tool for better monitoring that would improve the personalization of the treatment and, thus, its effectiveness.

APPENDIX C: ECONOMIC BUDGET

This appendix contains an estimation of the budget that would be necessary to Perform this thesis taking into account direct and indirect costs. It takes into account that the average salary of person with a degree in Finland would be paid 20 €/h and the general tax is 24%. The thesis took about six months to perform. Since it is of 12 ECTS, it corresponds to approximately 325 hours of work.

WORKFORCE COST (Direct Cost)

Hours	Salary/hour	Total
325	20 €	6500 €

RESOURCE MATERIAL COSTS (Direct Costs)

	Purchase price	Use (months)	Amortization (years)	Total
Personal computer (Software included)	1300 €	6	4	162.50 €
Suunto Movesense ® gyroscope sensors	40 €	12	2	20 €
Smart insole Forciot ®	1000 €	12	2	500 €

TOTAL MATERIAL COSTS

682.50 €

GENERAL EXPENSE (Indirect Costs)

15%

Over DC

1077.38 €

INDUSTRIAL BENEFIT

6%

Over DC+IC

495.59 €

SUBTOTAL BUDGET

8755.47 €

APPLICABLE TAX

24%

2101.31 €

TOTAL BUDGET

10856.78 €